Manganites: phenonmenology, present understanding and future prospects

Sandeep Pathak*

Materials Research Center, Indian Institute of Science, Bangalore - 560 012, India

(Dated:)

Manganites are mixed-valence manganese oxides $Ln_{1-x}A_xMnO_3$ (Ln = rare-earth cation, A = alkaline earth cation), with perovskite structure. These compounds exhibit a rich variety of crystallographic, electronic and magnetic phases. Resistivity of manganites samples reduces by a "colossal" factor as large as 10^7 on application of few Tesla magnetic field. This effect is named as *Colossal Magnetoresistance (CMR)*. The strangest thing about manganites is that even single crystals of high chemical purity exhibit electronic phase separation where in "phases" of different electronic and magnetic properties coexist. Even these coexisting phases can be electronically inhomogeneous at nanoscopic length scales. Generally, CMR is accompanied by such inhomogeneties. This review gives an account of the literature on manganites, discussing phenomenology, present thoeretical understanding and future prospects.

I. INTRODUCTION

Jonker and Van Santen[1] reported ferromagnetism in doped manganites, $Ln_{1-x}A_xMnO_3$ (Ln = rare-earth cation, A = alkaline earth cation), in 1950. This field has been investigated extensively since then. The field had become obsolete until the discovery of CMR effect [2–4] in 1990's. Despite of considerable research effort, theoretical understanding of the manganites is far from complete.

Manganites are important from the technological point of view because of colossal magnetoresistance(CMR) effect. The CMR effect(FIG. 1) is the decrease in resistance on application of magnetic field. Decrease can be as large as a factor of 10^7.

Manganites show complex electronic and magnetic properties and very rich phase diagram. Almost all the degrees of freedom known in solid state physics, namely itinerant charges, localized spins, electronic orbitals and lattice vibrations, are at play. Various ground states are possible as a function of doping, x and temperature, T. Manganites show insulating states which can be paramagnetic(PI), ferromagnetic(FI) as well as anti-ferromagnetic(AFI). PI state is a big surprise. Generally, a metal at high temperatures is paramagnetic. Under certain conditions, in AFI state,

*sandeep@mrc.iisc.ernet.in

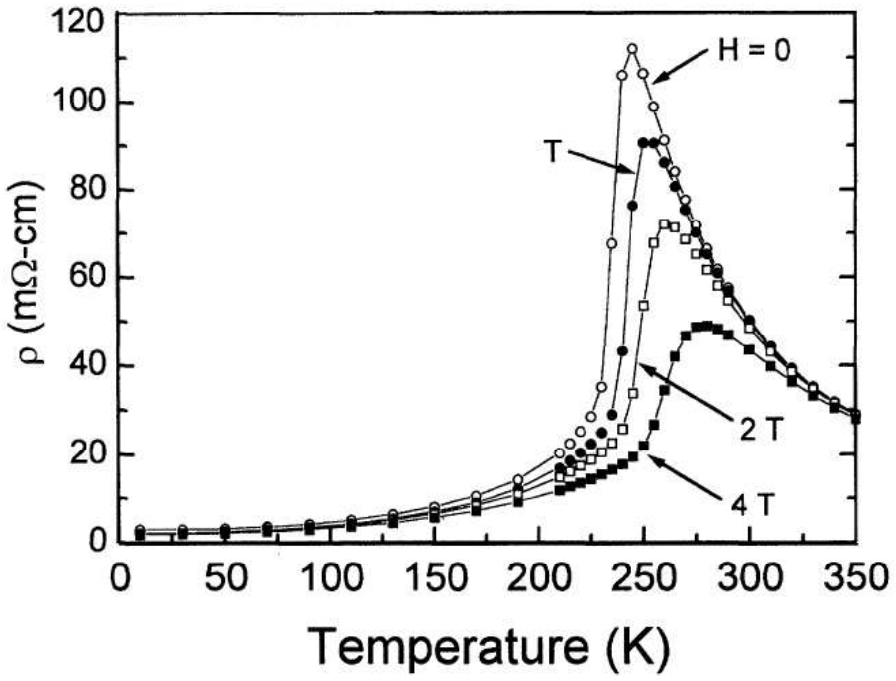

FIG. 1: Resistivity of $La_{0.75}Ca_{0.25}MnO_3$ sample as a function of temperature for vaious fields[5].

electrons get localized in particular order in the crystal. This state is named as charged ordered insulator (COI). There are metallic states, both paramagnetic(PM) and ferromagnetic(FM).

The strangest and most exotic thing about manganites is that even in single cystal sample of high chemical purity, these states with different electronic and magnetic property can coexist at different locations in the sample. This is called phase separation(FIG. 2) and it arises because the magnetic, electronic and crystal structure strongly interacts with each other in manganites. Phase separation in manganites occur at various length scales ranging from sub-nanometers to up to even few microns. Even stranger thing about manganites is that even a pure phase can be electronically inhomogeneous e.g. a ferromagnetic phase can be charged ordered at nanoscopic length scale[6]. Thus, manganites are intrinsically inhomogeneous. This is believed to be because of strong correlations. Large fraction of community believes that PS is the cause for CMR. This is still an open question and more work is required to prove or disprove the belief.

Manganites have perovskite structure (FIG. 3), similar to $CaTiO_3$. Electronic configuration of manganese is $[Ar]3d^54s^2$. Mn ion is in the octahedral field of six oxygen ions. The degenerate d-orbitals of Mn ion splits up into two: two degenerate e_g orbitals(d_{z^2}, $d_{x^2-y^2}$) higher in energy than three degenerate t_{2g} orbitals(d_{xy}, d_{yz}, d_{zx}) due to crystal field splitting(FIG. 4). Mn^{3+} has 4 electrons in d-orbitals. Each of three t_{2g} orbitals accomodate one electron each and one of two

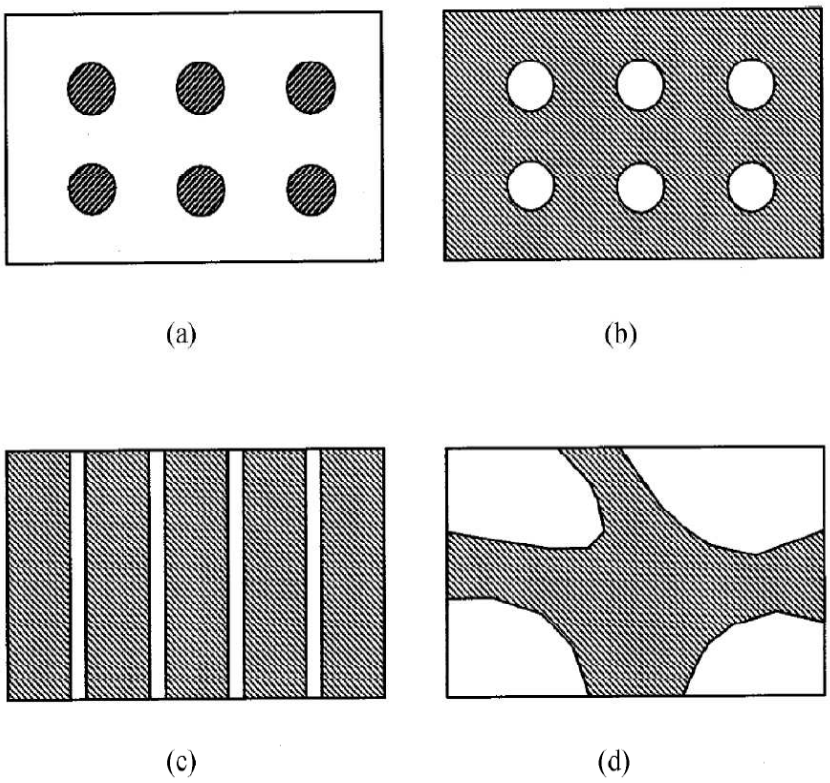

FIG. 2: Electronic phase separation (a) ferromagnetic (conducting/metallic) droplets in an insulating background, (b) a conducting state where a ferromagnetic (conducting) part of the crystal has separated (insulating) droplets, and (c) charge-stripes, a macroscopic phase separation state is shown in (d). Hatched portions represent the ferromagnetic regions with high carrier concentration (and are therefore conducting)[7].

e_g orbitals accomodate one electron. The t_{2g} electrons, due to strong Hund's coupling, lock into a "core spin" with S = 3/2. The extra e_g electron is free to hop in the crystal. These energy levels further splits up due to John- Teller distortion. Thus, there is one itinerant electron and a "core spin" of S = 3/2 per site of parent $LaMnO_3$ compound. When x fraction of La^{3+} are replaced by a divalent ion, it is equivalent to doping system with holes which have fraction x.

This review contains the manganites phenomenology, theoretical understanding and lists solved and unsolved issues in the field. Lots of excellent review articles and books are dedicated to these exotic class of materials [7–25]. Plan of this review is as follows. Phenomenology is presented in section II. Section III discusses the theory of manganites. Present understanding is reported in section IV by listing solved and open issues in the field. Finally, the article is concluded with author's outlook towards manganites in section V.

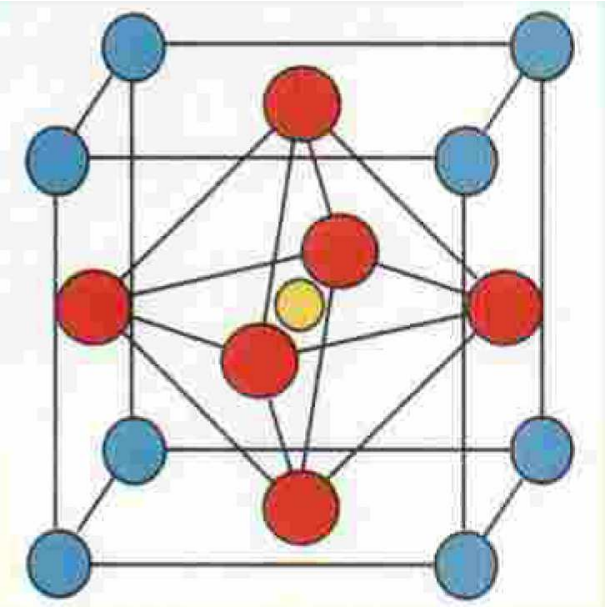

FIG. 3: Unit cell of perovskite $LaMnO_3$: trivalent rare earth and divalent rare alkaline earth cations occupy corners of the cube(blue), Oxygen ions(red) occupy face centers while $Mn^{3+/4+}$ occupy cube center. Figure taken from [8].

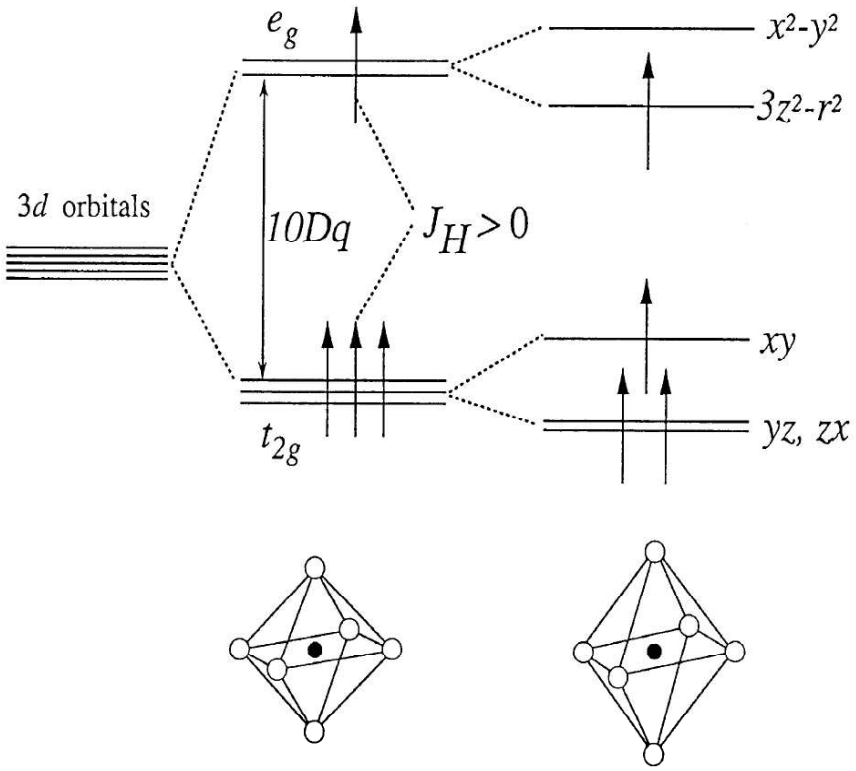

FIG. 4: Crystal field splitting of the five-fold degenerate atomic 3d levels into lower t_{2g} and higher e_g levels. The particular Jahn-Teller distortion shown lifts each degeneracy as shown. Figure taken from [9].

II. PHENOMENOLOGY

Manganites can be broadly classified into three classes, namely large, intermediate and low bandwidth manganites. This classification is on the basis of magnitude of hopping amplitude for e_g electrons. Larger the amplitude(bandwidth), more metallic the manganite should be. Large bandwidth manganites show a ferromagnetic metal(FM) phase. FM state tends to be less prominent as bandwidth is reduced. Bandwidth can be tuned by applying pressure, changing size of the ions, etc. and so is the change in phenomenology as we will see in detail below.

A. Large Bandwidth Manganites

$La_{1-x}Sr_xMnO_3$ falls into this category. As mentioned, it is believed that magnitude of hopping amplitude for e_g electrons is large in these compounds. These compunds have large Curie Temperature, T_c, which makes them good candidates for applications. FIG. 5 shows the resistivity measurement for this compound for various dopings[26]. Metallic regime can be identified with regime where $\partial\rho_{dc}/\partial T > 0$. Clearly there is metal-insulator transition for $x > 0.175$. Phase diagram(FIG. 6) is produced from the transport measurements [26–28].

1. Discussion of Phase diagram

- *Canted Insulator*: Parent $LaMn0_3$ is an AF insulator. Transition from AFI to ferromagnetic metal occurs via canted insulating(CI) state(FIG. 7). It is similar to a state produced by a magnetic field acting over an anti-ferromagnet. Spins develop a moment in one direction, while being mostly antiparallel within the plane perpendicular to that moment. There are doubts, on theoretical grounds, whether canted state exist, instead, it is believed that AF and FM states coexist. This is an open issue.

- *Ferromagnetic Insulator(FI)*: This phase[29] exists in a narrow range between CI and FM states and at low temperatures. There are evidence of charge ordering(PS) in this regime[30].

- *Paramagnetic Insulator(PI)*: This is by far the most unexpected phase displayed by manganites. Paramagnetism is generally accompanied by metallicity. It converts to metal at low temperatures which is a common characteristic of all bandwidth manganites.

- *Metallic Regime*:

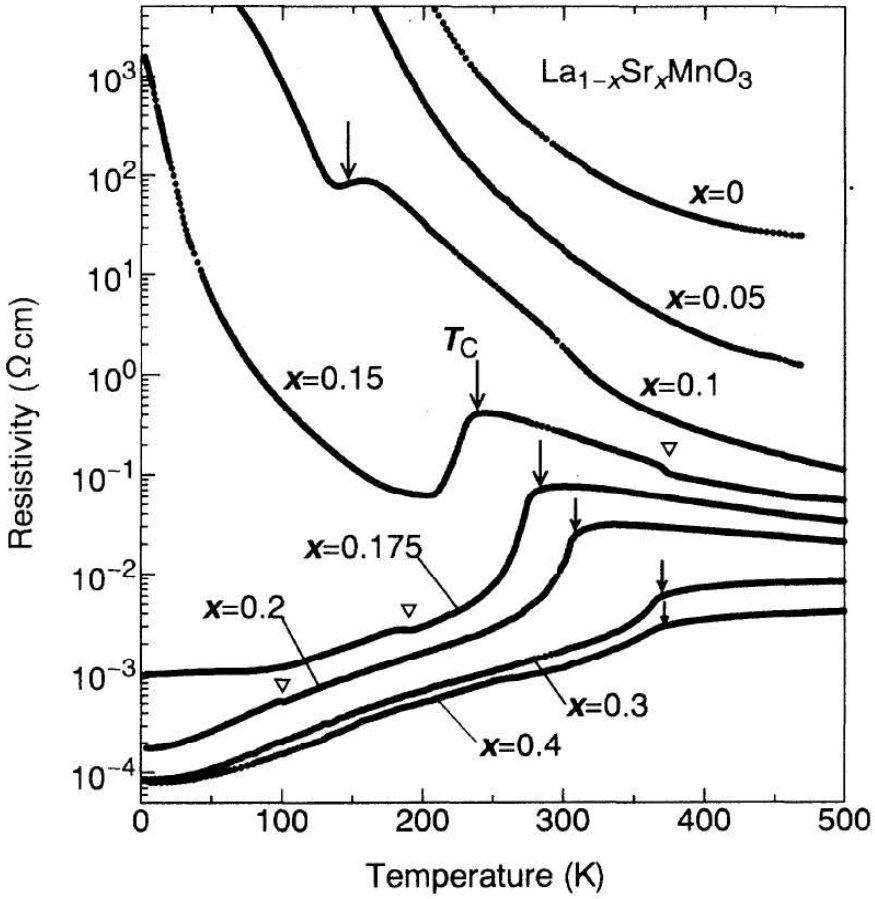

FIG. 5: Temperature dependence of resistivity for various single crystals of $La_{1-x}Sr_xMnO_3$. Arrows indicate the ferromagnetic transition temperature, T_c[26].

- Paramagnetic metal ($x > 0.3$, $T > T_c$)
- Ferromagnetic metal ($0.175 < x < 0.5$): This phase is a poor metal. There is strong ferromagnetic Hund's coupling between itinerant e_g electrons and t_{2g} core spin. An electron can easily hope from site to site, if the core spins are aligned ferromagnetically. Hopping takes place via oxygen p-orbitals by mechanism called "double exchange (DE)" [31], described in more details later.
- Anti-ferromagnetic metal ($x > 0.5$): AF is A-type where there is ferromagnetism in planes and antiferromagnetism between those planes(for various kinds of magnetic order, see FIG. 8). There is uniform $d_{x^2-y^2}$-type orbital order within ferromagnetic planes(FIG. 9).

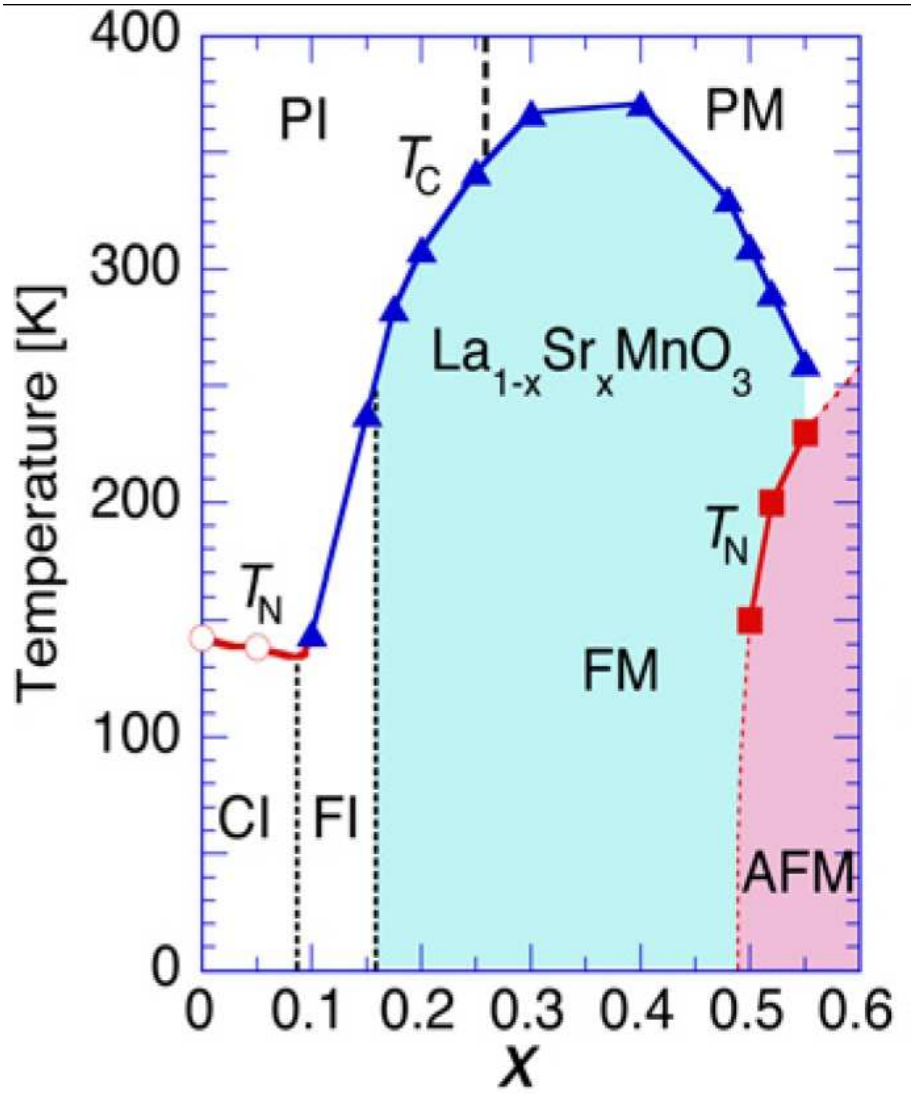

FIG. 6: Phase diagram of $La_{1-x}Sr_xMnO_3$ prepared with data from [26–28]. The AFM phase at large x is an A-type AF metal with uniform orbital order(See text for more details). PM, PI, FM, FI, and CI denote paramagnetic metal, paramagnetic insulator, FM metal, FM insulator, and spin-canted insulator states, respectively. T_c is the Curie temperature and T_N is the Neel temperature. Figure taken from [24].

2. CMR effect and phase separation

MR effect is maximized in the density regions separating the insulating from metallic states[11, 33, 34]. It is at these boundaries ,where the tendencies to form coexisting clusters and percolative transitions are the most important. This makes one think- are electronic inhomogenities necessary for CMR or whether inhomogenities just happen to follow CMR? This is a debatable issue and more work is required before final story can be told.

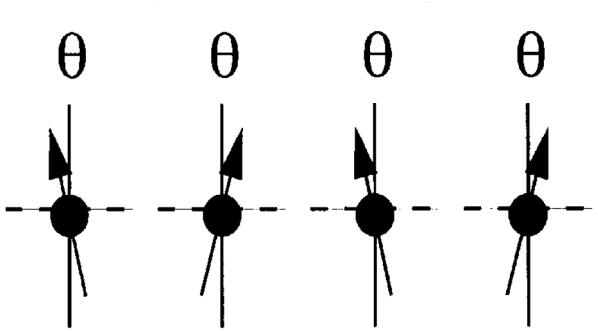

FIG. 7: Example of Canting.

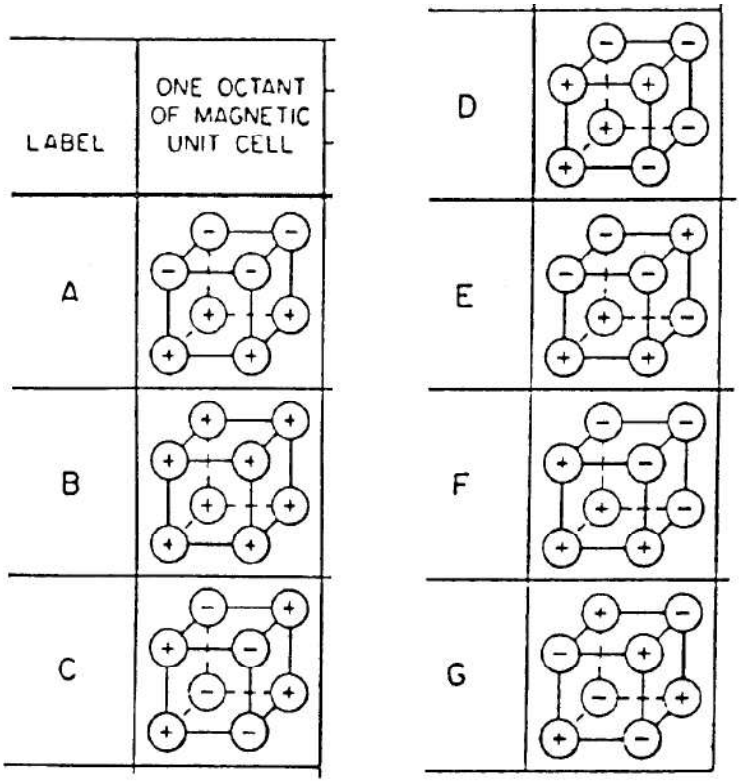

FIG. 8: Different type of magnetic structures. The circles represent the position of Mn ions, and the sign that of their spin projections along the z-axis. The G-type is the familiar antiferromagnetic arrangement in the three directions, while B is the familiar ferromagnetic arrangement.

B. Intermediate Bandwidth Manganites

These compounds show largest CMR effects, but Curie temperature, T_c is low. $La_{1-x}Ca_xMnO_3$ is one example of intermediate bandwidth manganites. It shows strong deviations from DE behaviour for example, more tendency for charge-ordering. There is FM phase, but in a narrow regime, that's why the terminology-intermediate.

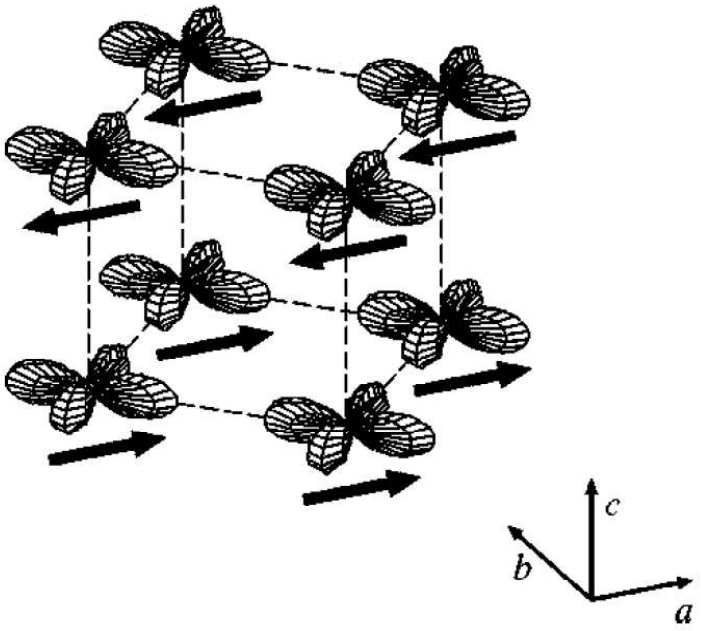

FIG. 9: Ordering of e_g orbitals in A-type anti-ferromagnetism [32].

1. CMR measurements

FIG. 10 shows one such experiment by Schiffer et. al.(1995) [5]. Curie Temperature, T_c and Metal-insulator transition temperature, T_{MI} are very close. This is a common characteristics of all manganites. CMR is very large, larger than 80%. The state is insulating above T_c, which is the reason for CMR. So, to explain CMR, one has to explain this insulating state. FM is partly explained by DE and there are signs of PS in FM state, as can be seen by large (30%) CMR in the regime.

2. Effect of hydrostatic pressure of transport

Bandwidth, W is expected to increase on application of hydrostatic pressure as hopping amplitude increases because ions come closer. This decreases dc resistivity, ρ_{dc}(FIG. 11). As W increases, DE mechanism comes to play and ferromagnetism is expected to be favored as can be seen by increase in T_c.

3. Phase diagram

Phase diagram(FIG. 12) is constructed from resistivity and magnetization measurements[36].

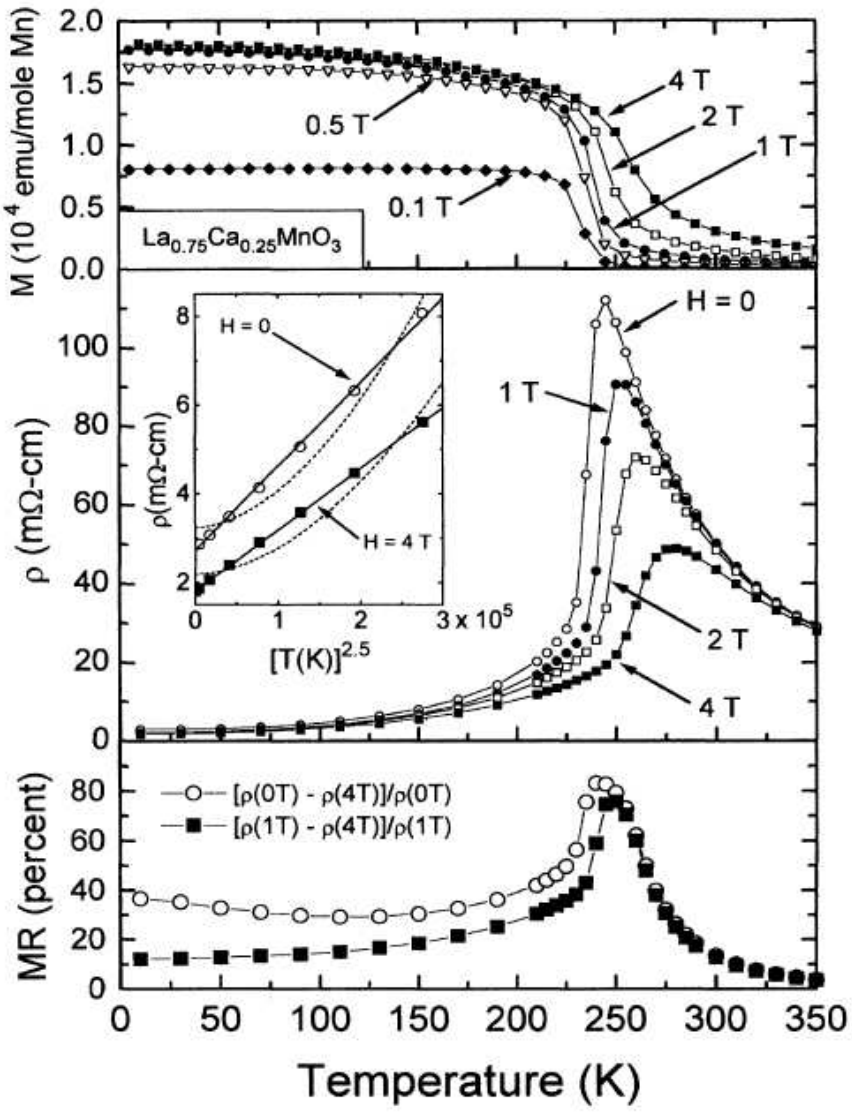

FIG. 10: The magnetization, resistivity and magnetoresistance of $La_{0.75}Ca_{0.25}MnO_3$ sample as a function of temperature for various fields[5].

- *Phase Separation:* FI and/or CAF could be spatially inhomogenous states with coexisting FM and AF states.

- *Ferromagnetic metal:* FM phase occupies just a fraction of the whole phase diagram. This suggest that DE does not give the full picture of manganites physics.

- *Charged ordered insulator:* Experiments[37] and thoeretical predictions[38] emphasise strong *electron-phonon coupling* in this regime.

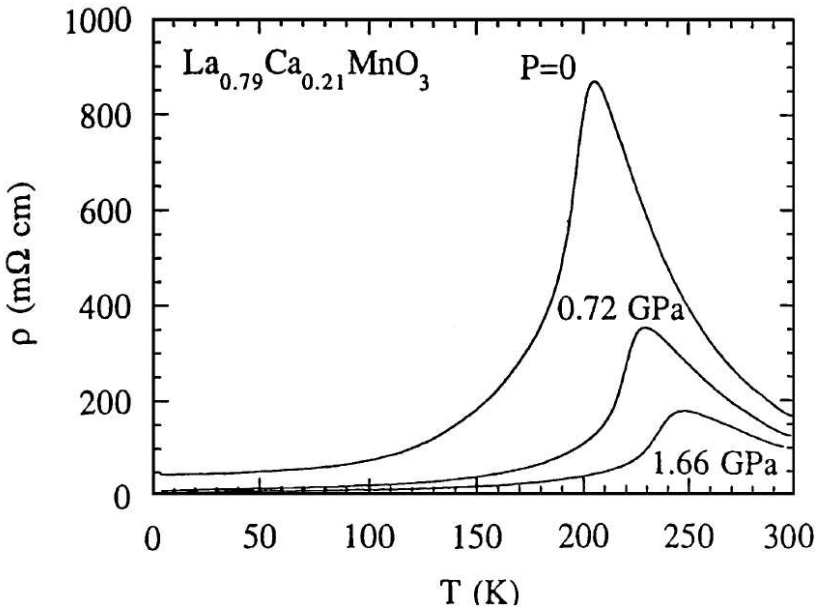

FIG. 11: The resistivity of $La_{0.79}Ca_{0.21}MnO_3$ sample as a function of temperature for various values of hydrostatic pressure [35].

- *CMR* There is no MR effect well inside the CO regime. CO state is very stable, even to the magnetic fields upto 12 T.To have CMR, density should be closer to the transition regime between FM and COI as emphasised before.

- *Commensurate densities:* It can be observed that there are well defined features at commensurate densities ($x = N/8, N = 1, 3, 4, 5, 7$)

- *Most optimal density for Ferromagnetism:* Curie temperature, T_c is maximum for $x = 3/8$. This is an "UNIVERSAL" phenonmenon as it is observed in $La_{1-x}Sr_xMnO_3$ as well[36]. This result is even contrary to the predictions of the "one-orbital DE" model and thus, this suggest that DE description is not sufficient to explain manganites physics.

- *Isotope effect:* By using different isotopes of oxygen, it was found that T_c shifts by as much as $20K$[39, 40]. This suggest strong electron-phonon coupling. Thus, it seems that electron-phonon coupling is crucial to the manganites physics apart from DE ideas.

- *Electron-hole asymmetry.*

- *Charge/Orbital Order:*

  - $x = 0$: A-type orbitally ordered spin state is stabilised(FIG. 13(a)).

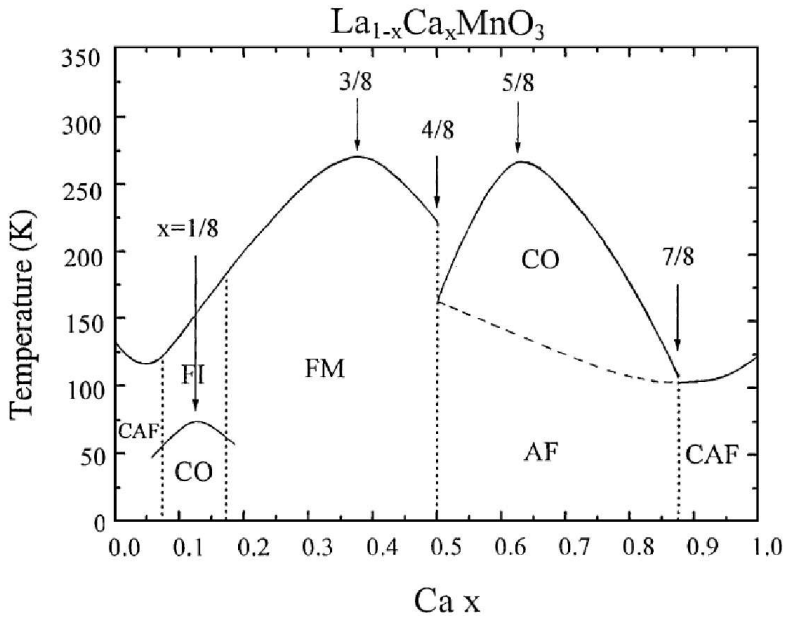

FIG. 12: Phase diagram of $La_{1-x}Ca_xMnO_3$ taken from [36]. FM: Ferromagnetic Metal, FI: Ferromagnetic Insulator, AF: Antiferromagnetism, CAF: Canted AF, and CO: Charge/Orbital Ordering. FI and/or CAF could be a spatially inhomogeneous states with FM and AF coexistence.

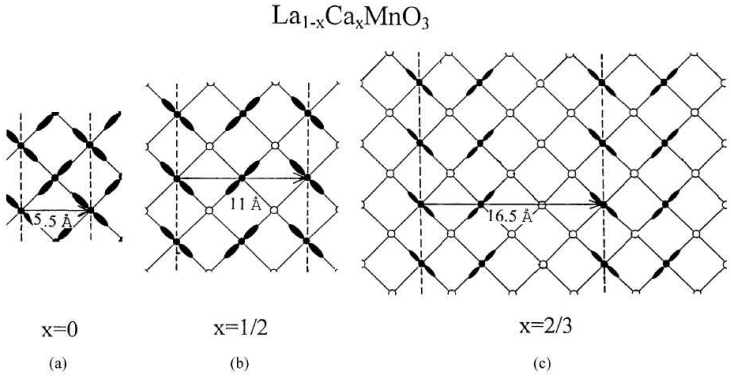

FIG. 13: The charge and orbital ordering configurations for $La_{1-x}Ca_xMnO_3$ with $x = 0, 1/2$, and $2/3$. Open circles are Mn^{4+} and the lobes show the orbital ordering of the e_g-electrons of Mn^{3+}. Figure taken from [36].

- $x = 0.5$: CE-type magnetic order is observed(FIG. 13(b)).
- $x = 2/3, 3/4$: A novel "bi-stripe" arrangement is stable(FIG. 13(c)).
- $x = 5/8$: Ground state is believed to be mixture of $x = 1/2$ and $x = 2/3$ configurations[36]. This is the phase separation scenario.
- $x = 1$: Ground state is G-type anti-ferromagnetic insulator.

C. Low Bandwidth Manganites

These compunds (for example, $Pr_{1-x}Ca_xMnO_3$) show maximum deviation from the standard DE ideas. Phase diagram is plotted in FIG. 14. A charge ordered (CO) insulating state is stabilized near $x = 0.5$, rather than a metallic phase contrary to large bandwidth compounds. Metallic ferromagnetic phase(FM) is not stabilized at zero magnetic field and ambient pressures. Ferromagnetic insulator (FI) phase is present in large region. Charge ordering is possible in this regime as predicted by some thoeretical calculations[41]. Anti-ferromagnetic charge ordered state is present in a large region of the phase diagram ($0.3 < x < 0.7$). Arrangement is CE-type(FIG. 13(b)) at $x = 0.5$[42]. For densities away from $x = 0.5$, arrangement can be assumed to that of defects in the CE state.

1. Effect of Magnetic field on the CO state

FIG. 15 shows the effect of magnetic field on CO state in $Pr_{1-x}Ca_xMnO_3$. The most interesting fact is that at finite magnetic fields, CO state gives way to ferromagnetic metallic state (FM), which is not stabilized at zero magnetic fields. At low temperatures, dc resistivity decreases by several orders of magntitude on applying few Teslas of magnetic field. Large CMR is observed and the possible reason is the percolation between CO and FM phase. The M-I transition is first order[43]. The behavior is similar for other hole densities as well(FIG. 16[44]). FIG. 17 shows that for densities larger than $x = 0.3$, larger field is required to destabilize CO state[43].

2. Effect of Pressure on the CO state

Pressure has the similar effect on the CO state as magnetic field(FIG. 18). FM state is favored over CO state at different conditions. This suggest that this FM-CO competition is crucial for understanding manganites physics.

3. Replacement of Ca by Sr

Consider compound of chemical composition, $Pr_{1-x}(Ca_{1-y}Sr_y)_xMnO_3$, where fraction y of Ca ions are replaced by Sr. It leads to similar effect as the effect due to magnetic field and pressure as a function of y. FIG. 19(a) shows the M-I transition for x=0.35 as a function of y. FIG. 19(b) shows that replacement of Ca by Sr decreases the critical field needed to stabilize FM phase[43]

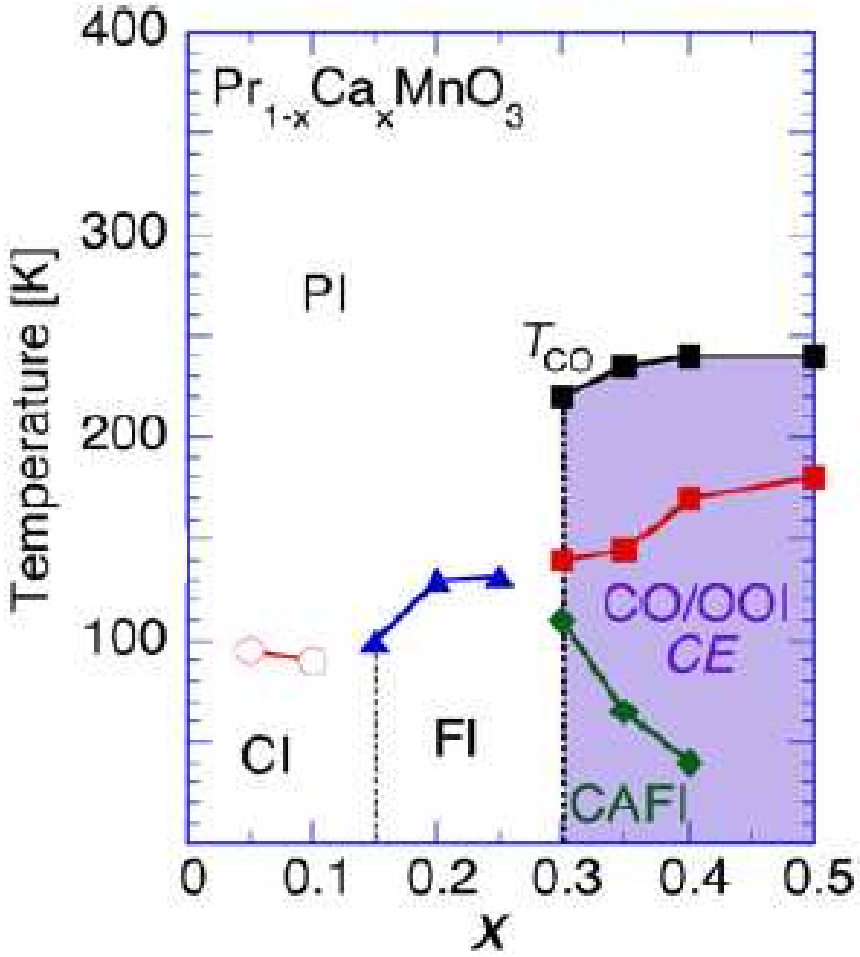

FIG. 14: Phase diagram of $Pr_{1-x}Ca_xMnO_3$. PI and FI denote the paramagnetic insulating and ferromagnetic insulating states, respectively. For hole density between 0.3 and 0.5, the antiferromagnetic insulating (AFI) state exists in the charge/orbital-ordered insulating (COI) phase. The canted antiferromagnetic insulating (CAFI) state, which may be a mixed FM-AF state, also has been identined between $x = 0.3$ and 0.4. Figure taken from [24].

as expected because of size of Sr. Effect of cation size is better described by tolerance factor to be described later.

D. Other Manganites

An interesting manganite is $Nd_{1-x}Sr_xMnO_3$ and its phase diagram[32] is shown in FIG. 20. Its phase diagram is quite similar to that of $La_{1-x}Sr_xMnO_3$, a large W compound, except that it has a stable CO state in tiny region around $x = 0.5$. Thus, it can be put into "intermediate"

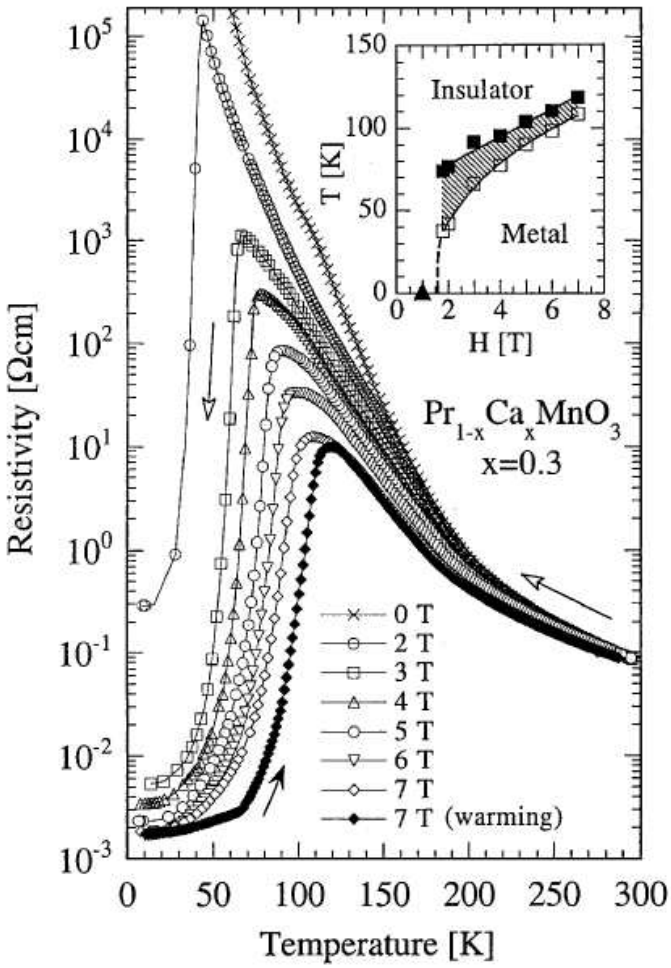

FIG. 15: Resistivity of $Pr_{1-x}Ca_xMnO_3$ with $x = 0.3$ as a function of temperature for various magnetic fields. Inset shows phase diagram in T-B plane. Hatched area is the hysteresis. Figure taken from [43]

W manganites category. There is a A-type AF metallic phase [46] with uniform $d_{x^2-y^2}$ orbital order in the ferromagnetic planes(FIG. 9). It is important and interesting because it shows the competition between FM and CO states with PS between them[47]. In $La_{1-z}Nd_z)_{1-x}Sr_xMnO_3$, the CO state does not appear until z less than 0.5[48]. Thus, FM vs CO character of a state at fixed state is determined by the size of the ions involved in the chemical composition. FIG. 21 shows an interesting relation between the average A-site radius, $< r_A >$ and the tendency to charge order. As $< r_A >$ decreases, tendency to charge order increases. CO phase is strongest for $Sm_{0.5}Ca_{0.5}MnO_3$ since (Sm,Ca) pair has the smallest $< r_A >$ (FIG. 22) for all the cation pairs shown in FIG. 21.

Finally, FIG. 23 shows phase diagram for different manganites (different cation pairs) for hole density, x = 0.45[49] on the temperature-$< r_A >$ plane. On one extreme, (La-Sr) compound show FM metallic state, while (Pr-Ca) compound show CO insulating state. One curious fact to be

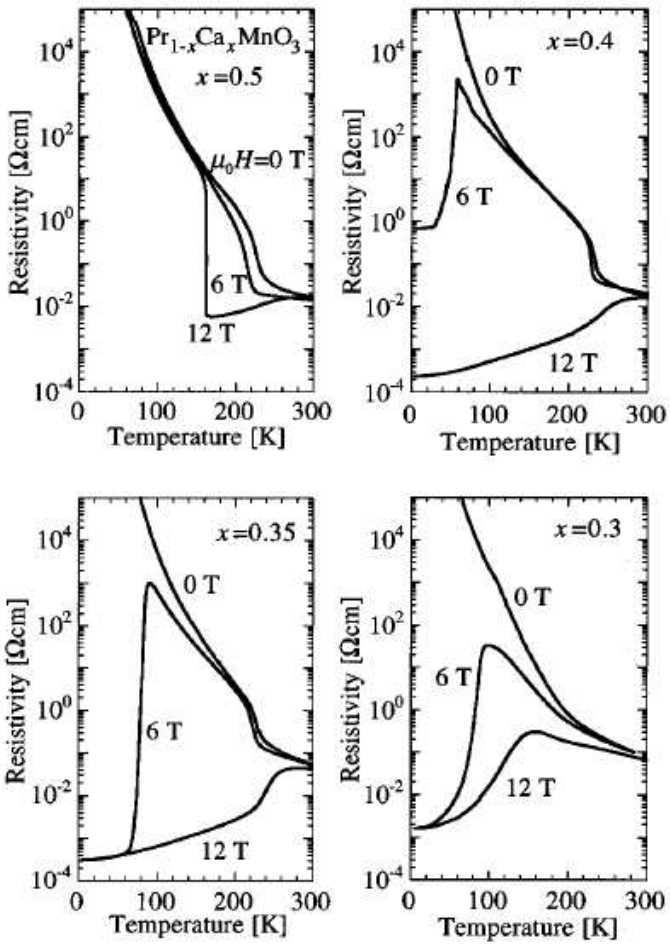

FIG. 16: Resistivity of $Pr_{1-x}Ca_xMnO_3$ as a function of temperature for various magnetic fields at various hole densities. Figure taken from [44]

observed is that T_{CO} and T_c, the two scales related to two totally different ground states have similar values. The better and equivalent description to average A-site cation radius is of tolerance factor as discussed below.

E. Importance of tolerance factor

It has been clear from the experiments discussed above that manganites physics is governed by the size of ions involved in the chemical composition of the manganites. A description by which we include A-site averaged ionic radius is that of tolerance factor. Tolerance factor, Γ is defined as:

$$\Gamma = \frac{< r_A > + r_O}{\sqrt{2}(r_{Mn} + r_O)}$$

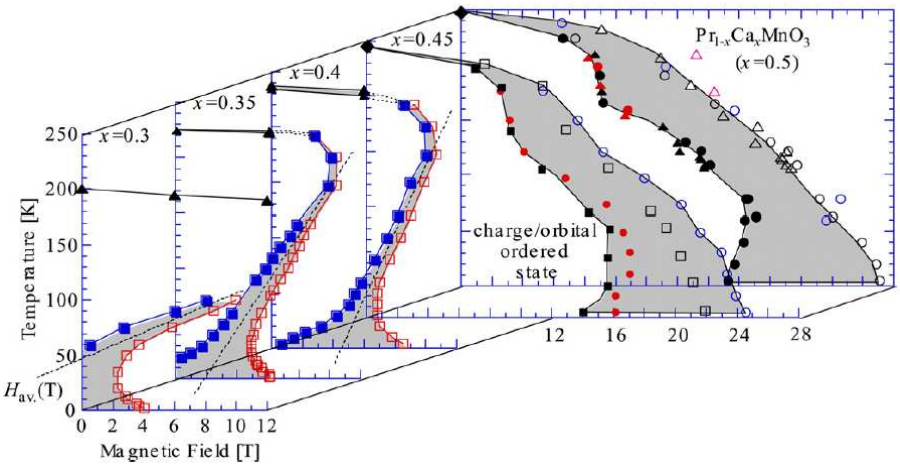

FIG. 17: The CO state of $Pr_{1-x}Ca_xMnO_3$ at several hole concentrations, plotted on the H-T plane. The hatched area indicates the hysteresis region. Figure taken from [43].

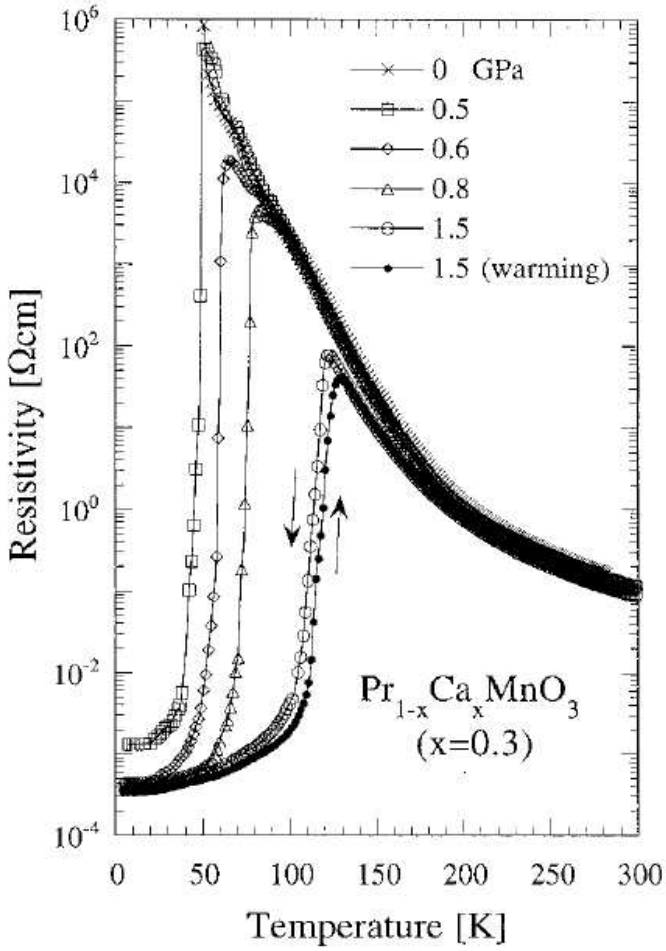

FIG. 18: Resistivity of $Pr_{1-x}Ca_xMnO_3$ with $x = 0.3$ as a function of temperature for various pressure values. Figure taken from [45]

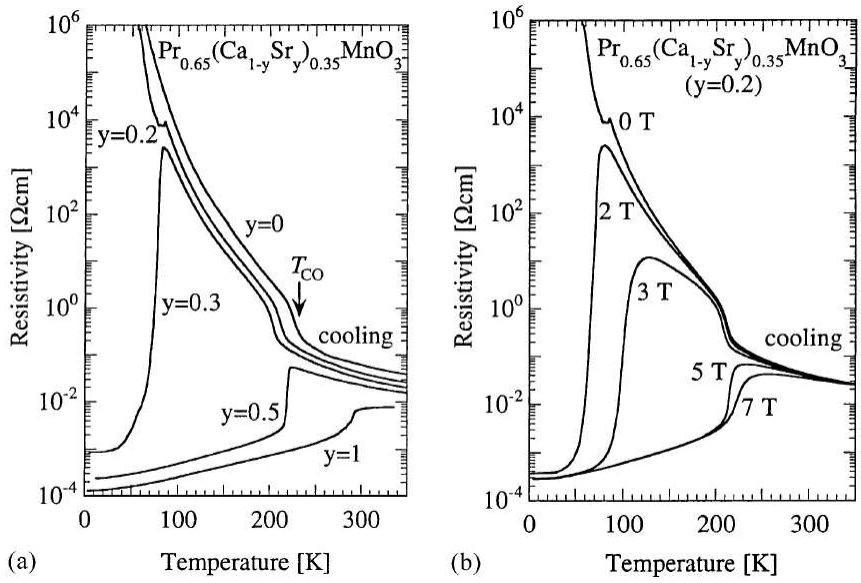

FIG. 19: (a) Dependence of resistivity on temperature for $Pr_{0.65}(Ca_{1-y}Sr_y)_{0.35}MnO_3$ for various values of y. (b) Resistivity vs. temperature of $Pr_{0.65}(Ca_{1-y}Sr_y)_{0.35}MnO_3(y = 0.2)$ for several magnetic fields. Figure taken from [43].

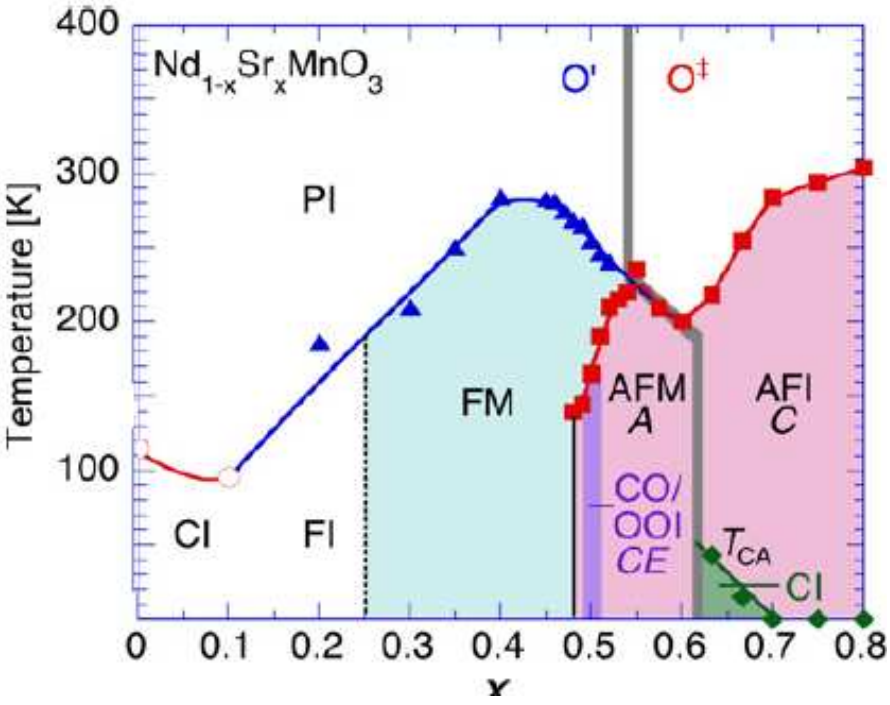

FIG. 20: Phase diagram[32] of $Nd_{1-x}Sr_xMnO_3$. The notation is standard. Figure taken from [24].

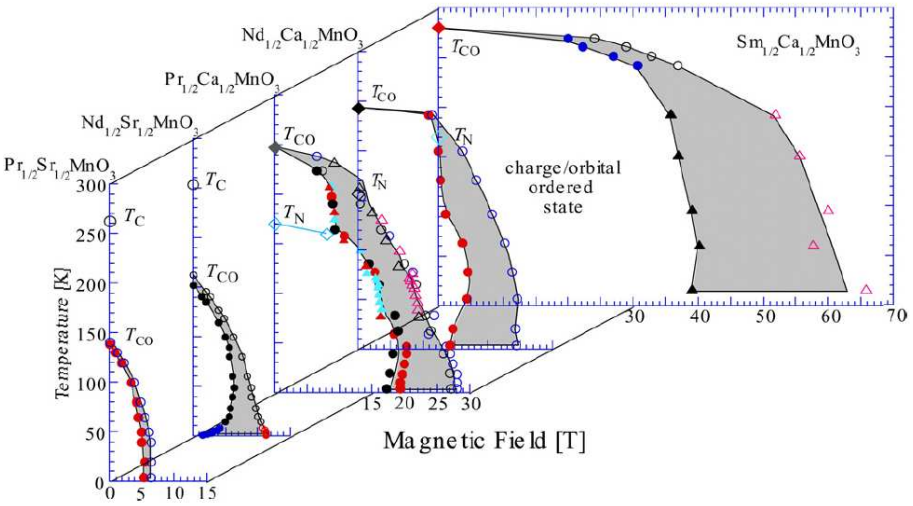

FIG. 21: The charge-ordered phase of various compounds $RE_{1/2}AE_{1/2}MnO_3$ plotted on the magnetic field-temperature plane. The hatched area indicates the hysteresis region. Figure taken from [24]

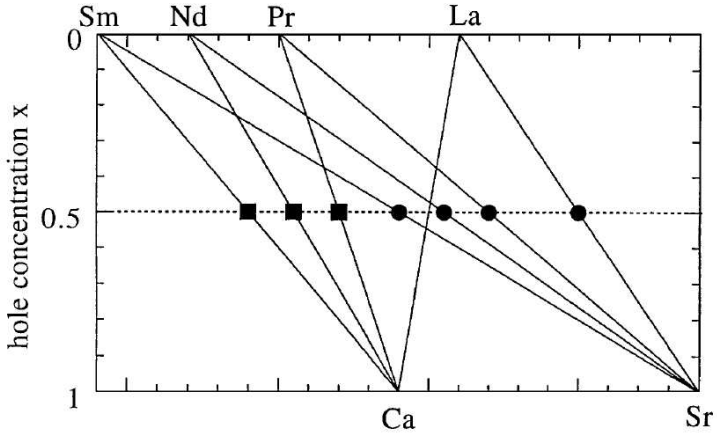

FIG. 22: Average ionic radius at x=0.5 corresponding to a mixture of a trivalent ion (upper abscissa) and a divalent ion (lower abscissa). Figure taken from [43].

For perfect cube, $\Gamma = 1$. If A site cations are smaller, $\Gamma < 1$. In that case, Mn-O-Mn angle θ becomes less than 180^o. This reduces the hopping amplitude (since DE includes hopping via p-orbitals of oxygen ion and the maximum hopping amplitude is possible for $\theta = 180^o$. If p-orbital points towards a Mn ion, it can not point directly to other Mn ion for $\theta \neq 180^o$.). Phase diagram of manganites is plotted in FIG. 24 on the temperature-tolerance factor plane.

Let's summarize our learning so far. Manganites physics seems to be governed by the competition between two totally different states, namely, ferromagnetic metal(FM) and charged ordered insulator(COI). Magnetic field drives a first order insulator to metal transition and thus, CMR

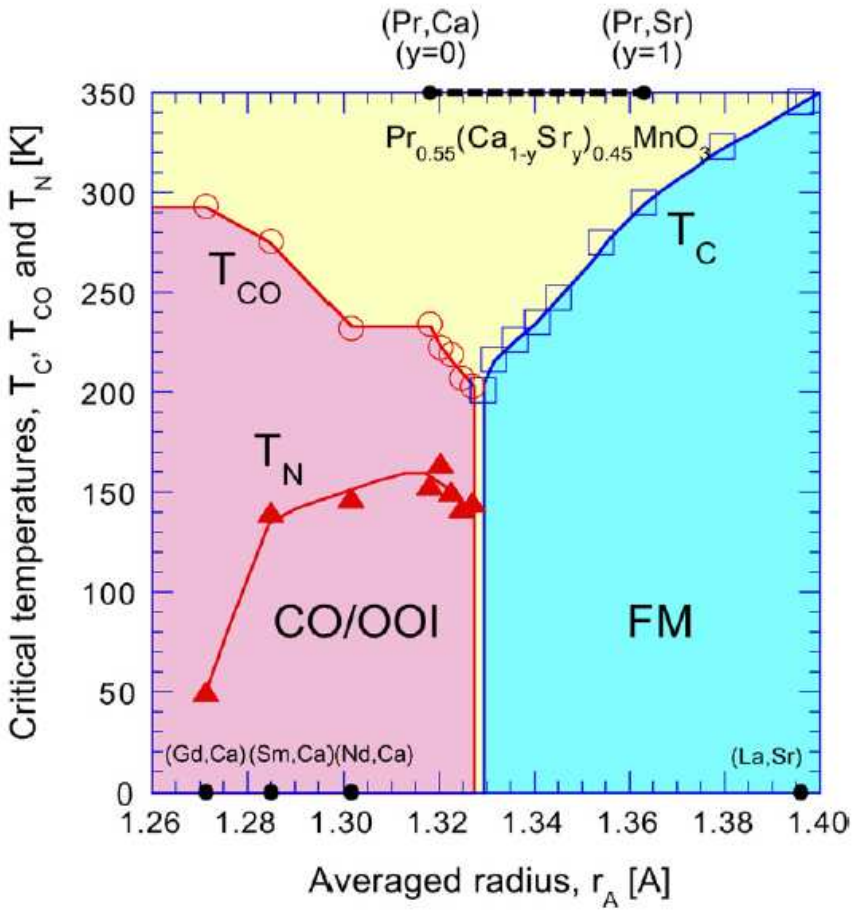

FIG. 23: The extended phase diagram[49] for x=0.45 over a wide regime of A-site averaged ionic radius. The notation is standard. Figure taken from [24]

effect is produced. Thus, stability of insulating charged order state to different external stimuli like magnetic field, pressure, strain(cationic size), disorder etc. has to be understood well to have a reasonable understanding of manganites. We now turn towards a recent development which has led to a debate all around as to what is the actual cause of CMR. The next section deals with phenomenology related to electronic inhomogenities in manganites.

F. Electronic inhomogenities in manganites

The most fascinating thing about manganites is that they are intrinsically electronically inhomogeneous[7, 8, 51, 52]. They show phase separation (PS) (FIG. 2) in which different "phases" having different electronic and magnetic properties coexist. The length scales of these inhomogeneties range from sub-nanometers to few micrometers. When one talks of phase separation, it is

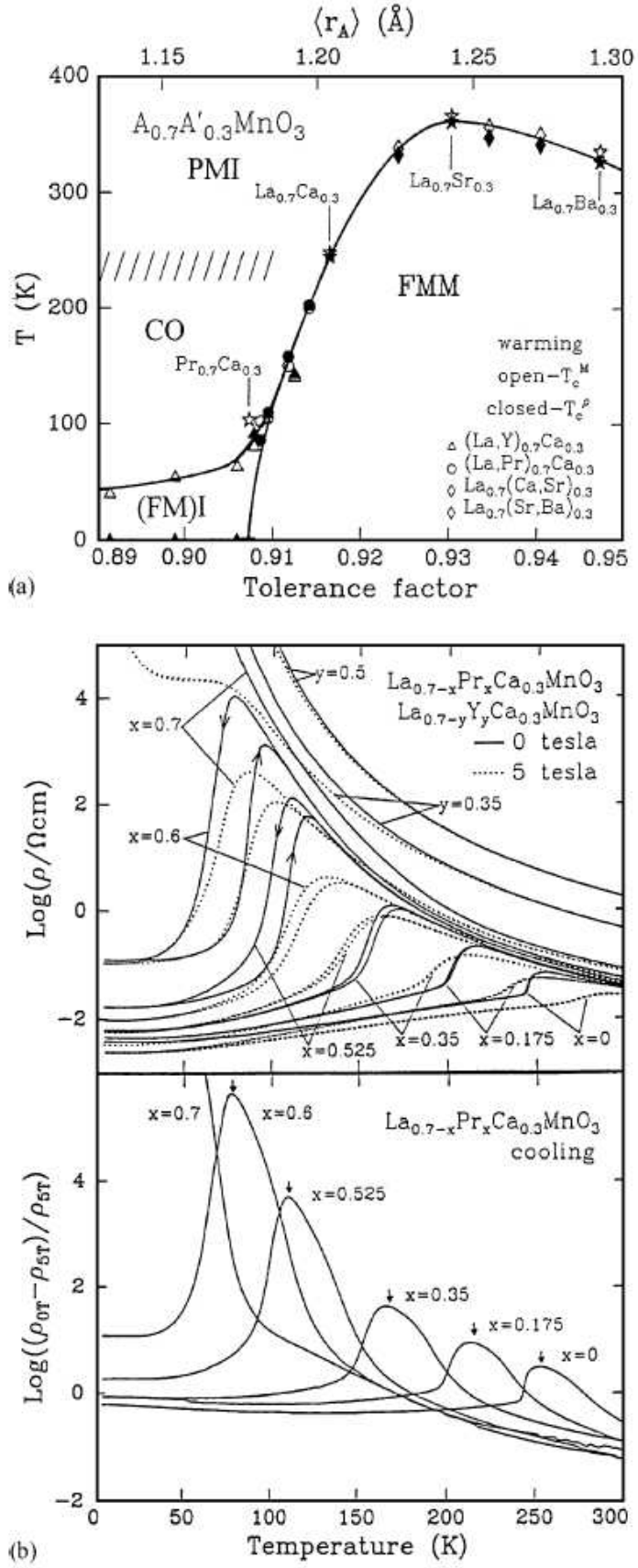

FIG. 24: Phase diagram of temperature vs. tolerance factor for the system $A_{0.7}A'_{0.3}MnO_3$, where A is a trivalent rare earth ion and A′ is a divalent alkali earth ion. Open and closed symbols denote T_c measured from the magnetization and resistivity, respectively. (b) Top panel: $\log \rho$(T) in 0 and 5 T for a series of samples of $La_{0.7-y}A'_yCa_0.3MnO_3$, with A′ mainly Pr but also Y. Bottom panel: MR factor. Figures taken from [50].

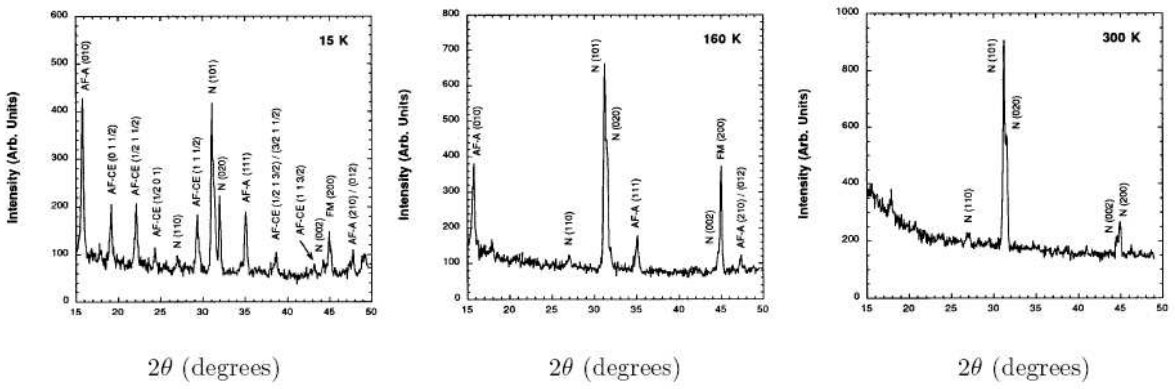

FIG. 25: Evolution of magnetic structure with temperature in $Nd_{0.5}Sr_{0.5}MnO_3$. At high temperatures (right most panel), the peaks are only nuclear indicated by N. As the temperature is lowered, magnetic peaks appear. AFM-A and AFM-CE represent, respectively, A-type and CE-type AFM structures, while FM indicates a ferromagnetic arrangement. Simultaneous presence of AFM-A, AFM-CE and FM peaks suggests "mesoscale" electronic inhomogeneities. Figure taken from [53]

implied that the inhomogeneties are on the mesoscopic length scales. These inhomogeneties may evolve on application of external stimuli like magnetic field, temperature etc. A large fraction of manganites community believes that they are essential for CMR effect, while there are people who believe that PS just happens to accompany CMR. There are evidences for both and in this section, we will explore these interesting phenomenon.

1. Neutron diffraction experiments

The first evidence for phase coexistence dates back to 1955, when Wollan et. al. reported both FM and AFM peaks in neutron scattering of $La_{1-x}Ca_xMnO_3$. Neutron diffraction studies of $Nd_{0.5}Sr_{0.5}MnO_3$[53] shows mesoscopic phase coexistence at low temperatures(FIG. 25). It displayed ferromagnetic state at 250K which transformed to A-type anti-ferromagnetic state at 220K and to CE type AFM state at 150K. At 15K, all such states coexist. Volume fraction of the three phases as a function of temperature are shown in FIG. 26(a). On application of magnetic field[54], ferromagnetic phase grows at the expense of anti-ferromagnetic phases(FIG. 26(b)). $Pr_{0.7}Ca_{0.3}MnO_3$ shows phase coexistence between a charge ordered AFM phase and a charge delocalize phase below T_{CO}. On field induced metallization, CO phase coexists with FM phase.

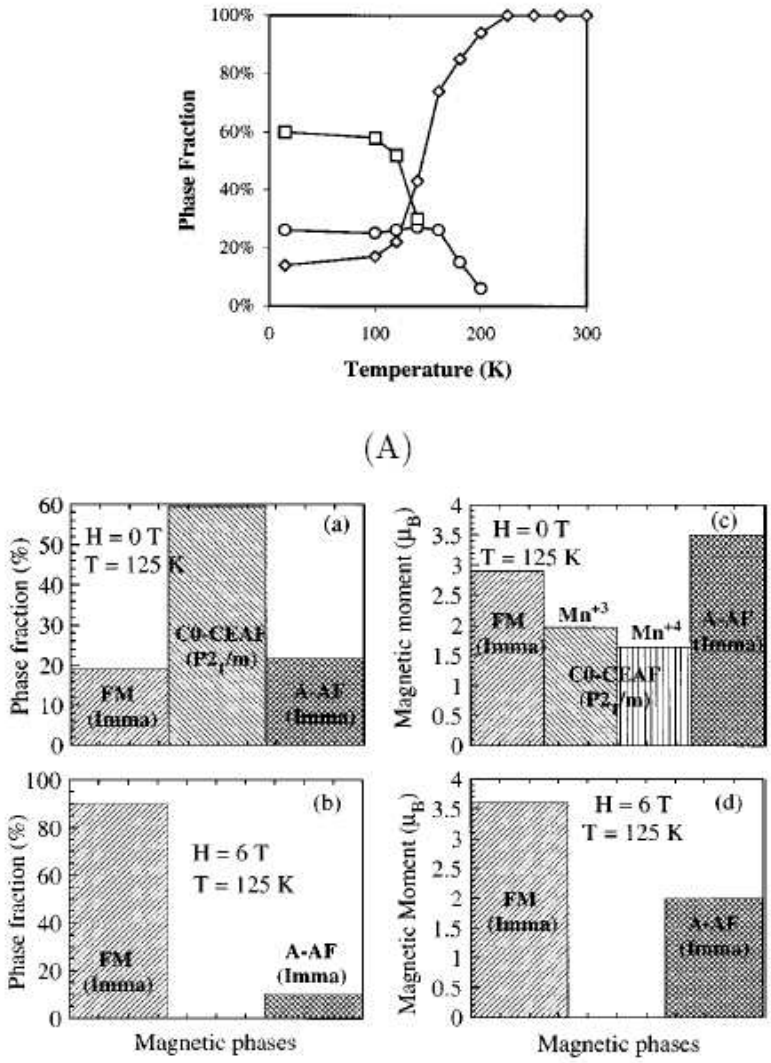

FIG. 26: (A) Volume fraction of phases as a function of temperature in $Nd_{0.5}Sr_{0.5}MnO_3$. Diamonds, circles and squares respectively represent ferromagnet (FM), antiferromagnet (A-type, A-AF) and antiferromagnet (CE-type, CO-CEAF) respectively. Figure taken from [53] (B) Phase fractions at 125K at different magnetic fields (a) 0T and (b) 6T; (c) and (d) show the magnetic moment in each of the phases. Figure taken from [54].

2. Magnetization and resistivity measurements

The magnetization and transport properties of $(La_{1-x}Ln_x)_{0.7}Ca_{0.3}MnO_3$ (where Ln = Nd, Gd and Y) shows mesoscopic phase separation[55]. Ln is used to control $< r_A >$. For $x < x_c$, magnetization measurements(FIG. 27(A), Ln = Nd) shows ferromagnetic transition with saturation magnetization of $3\mu_B$. For $x > x_c$, magnetization increases with decrease in temperature but never reaches the maximum value of $3\mu_B$. This suggest formation of CO phase coexisting with FM phase

for $x > x_c$. FIG. 27(A(b)) shows result of magnetization measurement for Ln = Gd, thus effect of decrease of $< r_A >$ on phase separation. This decreases x_c and T_c. Decrease in x_c implies that smaller favours phase separation and destablizes FM state(decrease in T_c) as expected. The resistivity measurements(FIG. 27(B)) shows that all three substitutions of Ln shows M-I transition below $x = x_c$. Inset shows the resistivity hysteresis across the transition. T_{M-I} decreases on doping and increases with $< r_A >$. Size disorder, which arises due to size-mismatch between A-site cations. This is quantified by a parameter, $\sigma^2 = \sum_i x_i r_i^2 - < r_A >^2$. Size disorder (increase in σ^2) favors PS and vice-versa[56](FIG. 27(C)).

3. Direct Imaging

It is possible to direct visual evidence of electron inhomogeneties using direct imaging probes like TEM, STM, MFM etc. The earliest evidence is of the discovery of charged stripes in $La_{1-x}Ca_xMnO_3$[57] with $0.5 < x < 0.75$ using TEM. There was alternative stacking of regions with Jahn Teller distorted oxygen octahedra surrounding Mn^{3+} ions and regions with Mn^{4+}-O_6 octahedra. The spacing was on the nanometer length scale.

STM study of $Bi_{1-x}Ca_xMnO_3$ with $x = 0.75$ revealed nanoscopic CO and FM domains[58]. TEM studies of $La_{5/8-y}Pr_yCa_{3/8}MnO_3$ demostrated coexisting CO regions with interspersed FM domains with a typical size of about $0.2\mu m$[59]. A mechanism for CMR was suggested as well. Spins in FM domains are randomly oriented. A spin polarized electron in one domain cannot hop to other domains in the absence of B due to unavailability of states. In the presence of magnetic field, the spins in different domains align and electron can hop from one domain to other unhindered and this decreases resistivity by a huge factor giving rise to CMR effect. Thus, in this view, PS is necessary for CMR effect. Scanning tunnelling spectroscopy studies[60] of $La_{0.7}Ca_{0.3}MnO_3$ showed that FM domains increases in size at the expense of insulating regions on application of magnetic field, thus supporting the above view about CMR of [59].

Magnetic force microscopy of $La_{1/3}Pr_{1/3}Ca_{1/3}MnO_3$[61] showed magnetic domains of mesoscopic scale evolving with temperature, also showing magnetic hysteresis which conincided with resistivity hysteresis. This experiment also suggested that PS may be crucial for CMR.

TEM studies of $La_{1/2}Ca_{1/2}MnO_3$ by [6] displayed mesoscopic domains of FM regions interspersed in insulating region. Some of FM regions were charged ordered(FIG. 28). This suggested that manganites are electronically inhomogeneous at nanoscopic length scales.

A recent experiment using photoemission spectro-microscopy of $La_{1/4}Pr_{3/8}Ca_{3/8}MnO_3$ de-

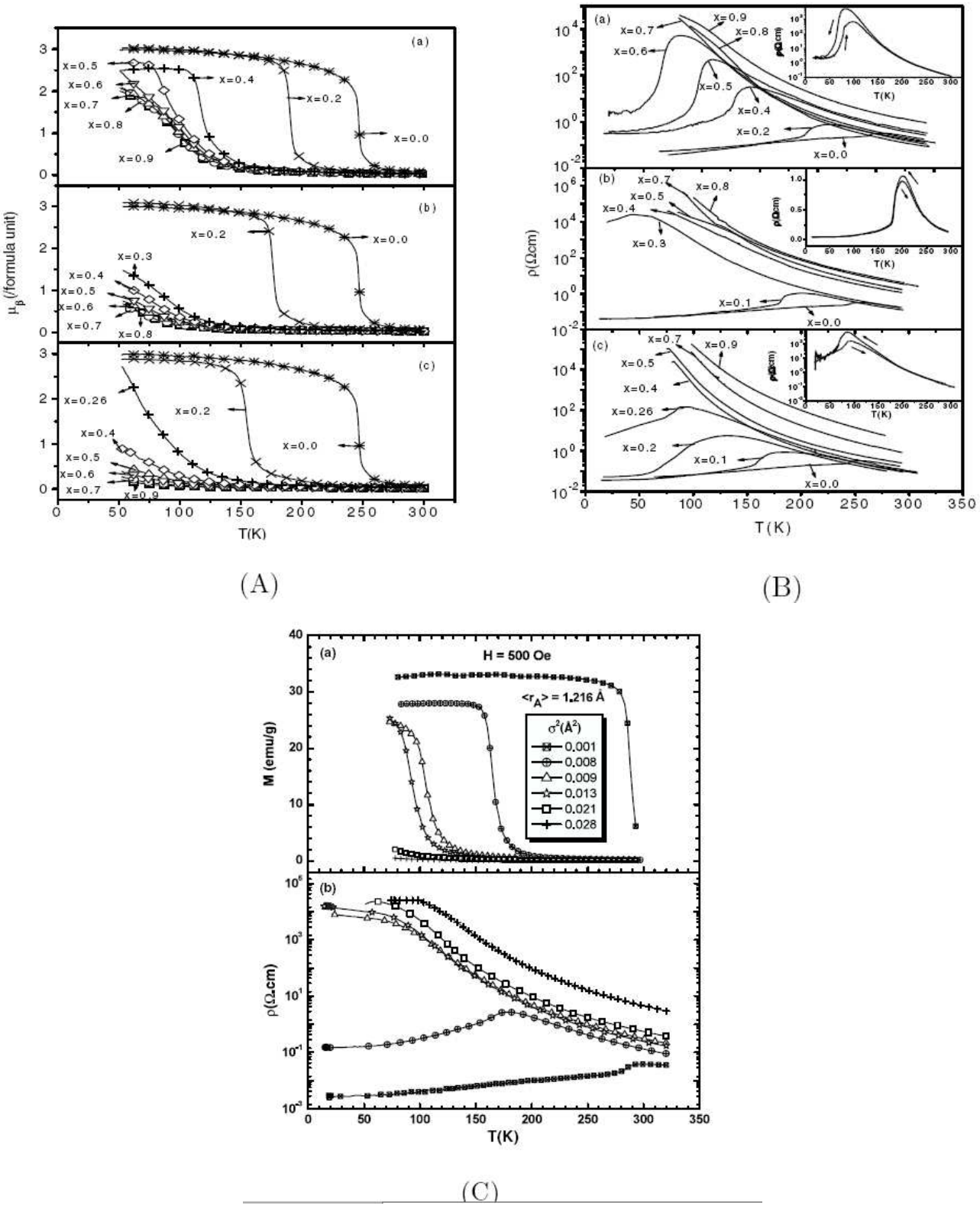

FIG. 27: (A) Temperature dependence of magnetization of $(La_{1-x}Ln_x)_{0.7}Ca_{0.3}MnO_3$. (B) Temperature dependence of the resistivity of $(La_{1-x}Ln_x)_{0.7}Ca_{0.3}MnO_3$. The insets show the resistivity hysteresis. In graphs in (A) and (B) panels (a), (b) and (c), respectively correspond to Ln=Nd, Gd and Y. Figures taken from [55] (C) Variation of magnetization (a) and resistivity (b) with temperature. The data shown is for $Ln_{0.7-x}Ln'_xA_{0.3-y}A'_yMnO_3$ with $< r_A >$ fixed. The different curves show results for different σ^2. Figure taken from [56].

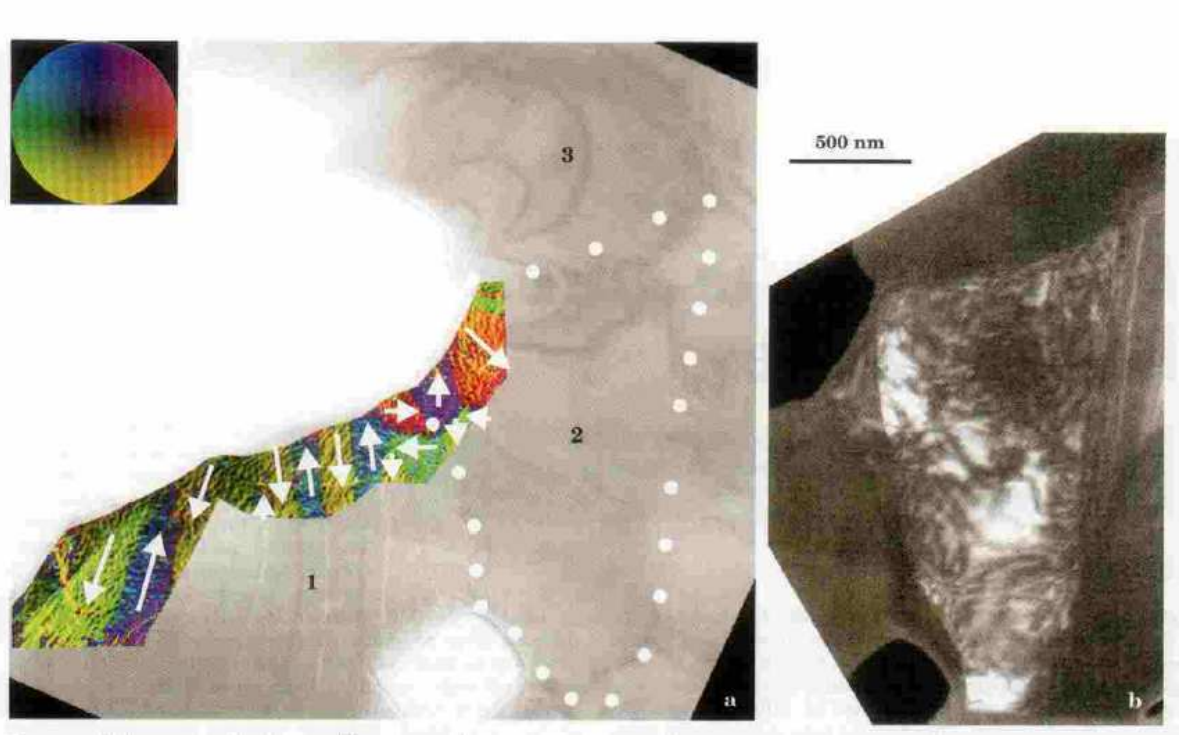

FIG. 28: $La_{1/2}Ca_{1/2}MnO_3$ is viewed with electron holography(color overlay) and TEM at 90K. (a) Three grains, numbered 1-3 are shown. Grain 1 is ferromagnetic, grain 3 is charge ordered with no net magnetic moment. (b) When viewed in dark, grain 2 shows nanoscopic bright regions showing strong charge order that coincides with the fully ferromagnetic domain seen in (a). Figure taken from [6].

mostrated large domains of insulating regions interspersed in a metallic background. The regions evolved on increasing temperature with metallic regions undergoing a metal-to-insulator transition at higher temperatures(FIG. 29). An interesting fact is that on cooling the sample back to low temperature, insulating regions seemed to be remembering where they were before heating. A memory effect!

III. THEORY OF MANGANITES

A. Important interactions in manganites

- *Hund's Coupling, J_H:*

  The parent compound $LaMnO_3$ has all manganese ions in the Mn^{3+} state. Mn^{3+} has four d electrons. Three electrons occupy low lying t_{2g} orbitals and electrons lock into a "core spin" with $S = 3/2$ due to strong Hund's coupling. The extra electron can occupy any of the two e_g orbitals (d_{z^2}, $d_{x^2-y^2}$) and its spin should also be preferentially parallel to the core spin

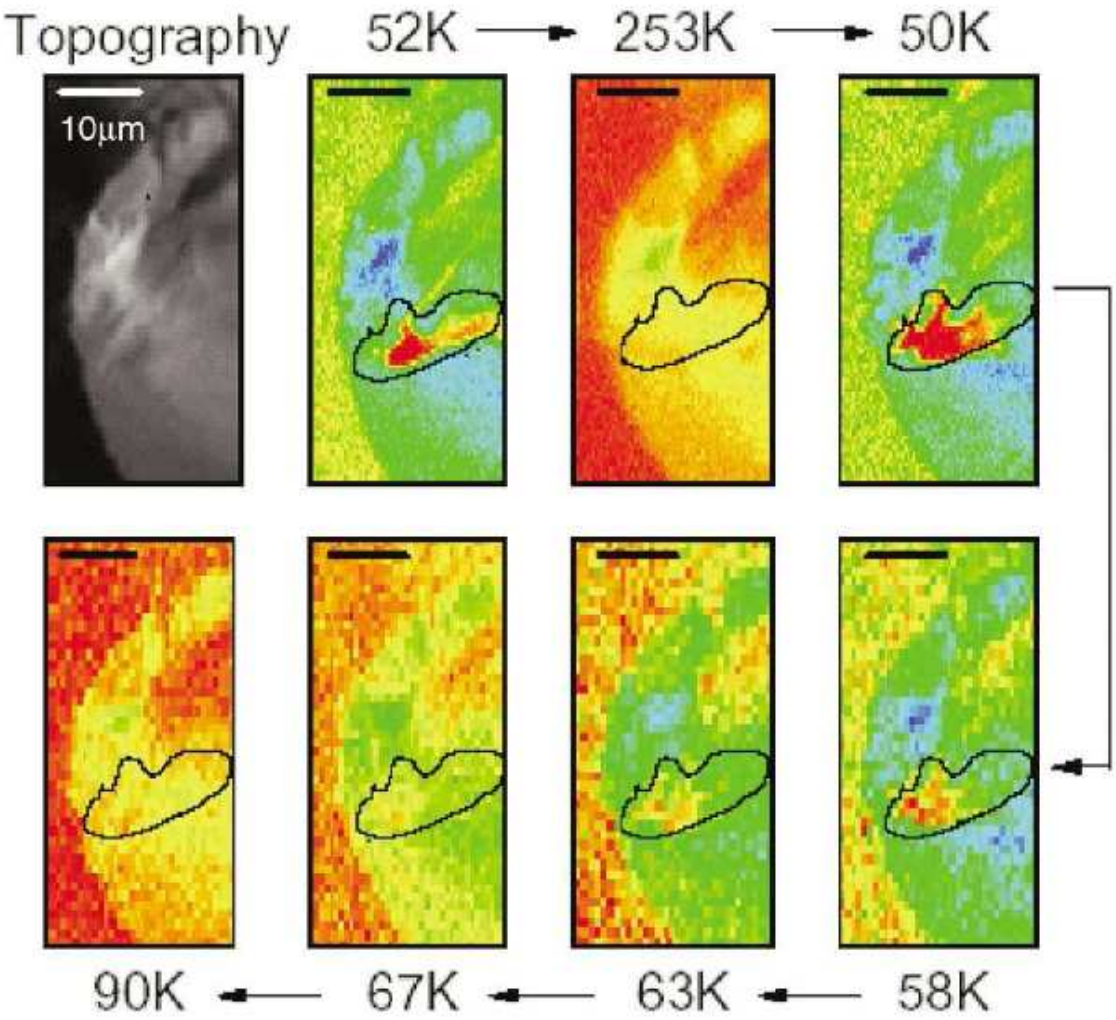

FIG. 29: Microscopic electronic inhomogeneities in $La_{1/4}Pr_{3/8}Ca_{3/8}MnO_3$. The indicated region represents a microscopic insulating patch of 15x5 μm^2. On warming the sample, the surrounding metallic regions become insulating. On cooling the sample, the insulating patch appears in essentially at the same locations (as was present before the warming process). Thus, the electronic inhomogeneties exhibit memory effects. On the length scale of $0.5\mu m$ (the spatial resolution) the material is chemically homogeneous. Colour key: Blue/green - metallic, Yellow-red - insulating.

because of Hund's rule. Hund's term in the Hamiltonian can be written as:

$$H_{Hund} = -J_H \sum_i \boldsymbol{S}_i . \boldsymbol{\sigma}_i$$

$$\boldsymbol{\sigma}_i = \sum_{\alpha\mu\mu'} c^\dagger_{i\alpha\mu} \boldsymbol{\tau}^{\mu\mu'} c_{i\alpha\mu'}$$

Here, $\boldsymbol{\tau}$ are the Pauli matrices in spin space, $\boldsymbol{S}_i$ is the t_{2g} spin at site i, and $c^\dagger_{i\alpha\mu}$ creates an

electron in the orbital state α, (=1,2 denoting the $d_{x^2-y^2}$, d_{z^2} orbitals respectively) and spin state μ (which can be up or down).

- *Hopping term, t:*

  Hopping from one Mn ion to its neighbor happens via p-orbital of oxygen ion. The mechanism is called "double exchange(DE)"[31](FIG. 30). It is a second order process[62] using an intermediate state with one hole on oxygen and both Mn ions in +3 oxidation state. The effective matrix element can be written as $t = t_{pd}^2/\Delta$, where t_{pd} is the matrix element for p-d hopping and Δ is the energy of the intermediate state which is typically much larger than t_{pd}. The hopping elements are different for different pairs of e_g orbitals and different for different directions in the crystal. The final effective tight-binding $e_g - e_g$ hopping Hamiltonian[63, 64] can be written as:

$$H_{KE} = -\sum_{<i,j>,\mu} t_{ij}^{\alpha\beta} c_{i\alpha\mu}^{\dagger} c_{j\beta\mu}$$

  Hopping is assisted if the core spins on two neighboring Mn ions are parallel. Thus, the simplest model for metallic ferromagnetism is obtained by combining H_{KE} and H_{Hund} and is commonly known as double exchange Hamiltonian:

$$H_{DE} = -\sum_{<i,j>,\mu} t_{ij}^{\alpha\beta} c_{i\alpha\mu}^{\dagger} c_{j\beta\mu} + \sum_{\alpha\mu\mu'} c_{i\alpha\mu}^{\dagger} \boldsymbol{\tau}^{\mu\mu'} c_{i\alpha\mu'}$$

- *John Teller Distortion:*

  One cannot get ferromagnetic insulating state within DE framework. Thus, there should be other interactions in the problem. The two e_g orbitals are degenerate. Consider elongation of the oxygen octahedron along the z-axis. Clearly, if an electron occupies d_{z^2}, the energy will be lowered. Thus, any distortion of the octahedron will reduce the energy of some linear combination of two e_g orbitals and increase the energy of other orthogonal linear combination. Energy of the system is reduced if orbital is preferentially occupied. Conversely, a preferential occupancy of an orbital will produce distortion of the octahedron. This is known as John-Teller effect. Let us label two e_g orbitals by 1,2(1,2 denoting the $d_{x^2-y^2}$, d_{z^2} orbitals respectively). Let elongation along z-axis is Q_z. Let energy change be proportional to distortion. Then, total energy change is given by

$$\Delta E = -gQ_z c_2^{\dagger} c_2 + gQ_z c_1^{\dagger} c_1$$

$$\Delta E = gQ_z \sum_{i\alpha\beta} c_{i\alpha}^{\dagger} \tau_{\alpha\beta}^{z} c_{i\beta}$$

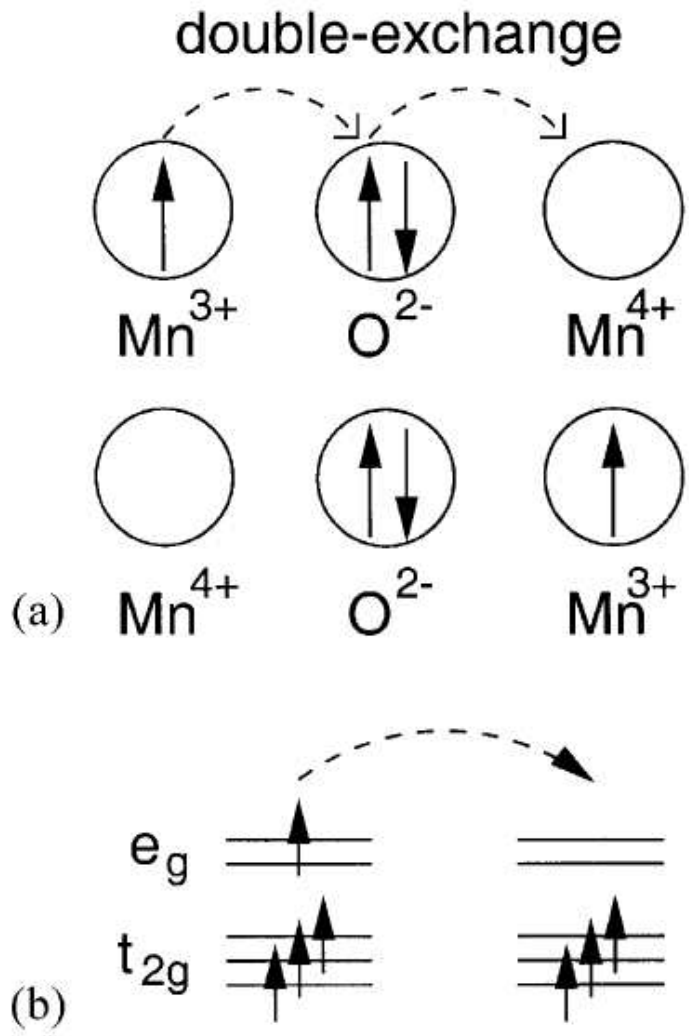

FIG. 30: (a) Double Exchange mechanism which two Mn and one O ion. (b) Mobility of e_g electrons increases if the neighboring spins are ferromagnetically aligned.

where, τ^z is a Pauli matrix. Thus, general John-Tellar term in the Hamiltonian can be written as:

$$H_{JT} = g\boldsymbol{Q}_i \cdot \sum_{i\alpha\beta\sigma} c^{\dagger}_{i\alpha\sigma} \boldsymbol{\tau}_{\alpha\beta} c_{i\beta\sigma}$$

Here, g is coupling constant, $\boldsymbol{Q}_i$ is the local lattice distortion, $\boldsymbol{\tau}$ are the Pauli matrices in spin space and $c^{\dagger}_{i\alpha\mu}$ creates an electron in the orbital state α and spin state μ (which can be up or down).

- *Lattice Energy:*

  Corresponding to these Jahn-Teller modes, the contribution to lattice energy by independent

harmonic oscillators is given by:

$$H_{lat} = \frac{1}{2}K\sum_i \boldsymbol{Q}^2 + \frac{1}{2M}\sum_i \boldsymbol{p}_i^2$$

- *On-site Coulomb interactions:*

  On-site coulomb interactions between e_g electrons is given by:

$$H_U = U \sum_{i\alpha\sigma\alpha'\sigma'} c^\dagger_{i\alpha\sigma} c_{i\alpha\sigma}(c^\dagger_{i\alpha\sigma} c_{i\alpha'\sigma'} - 1)$$

  This forbids two electrons occupying a site simultaneously.

B. Relative strengths of interactions:

- $t - 0.2eV$.
- $J_H - 2eV$
- $U - 5eV$ (often, ignored!)
- $J_{SE} - 0.02eV$ (AF super-exchange between two neighboring t_{2g} spins.)
- $E_{JT} - 0.5eV$

Large number of energy scales close in energy suggests a complex phase diagram. Also, manganites are expected to be extremely sensitive to external stimuli, as is the case in experiments.

IV. WELL UNDERSTOOD VS OPEN ISSUES

In this section, we list facts that are understood well and that are not well understood about the manganites[65].

A. Facts well understood

- At x=0,as in $LaMnO_3$, the ground state has staggered orbital order[64] and spins form an A-type anti-ferromagnet. Recently, a new FM charge-ordered phase was observed experimentally[6] and has been predicted in [66].
- At x=1, the arrangement is G-type anti-ferromagnet.

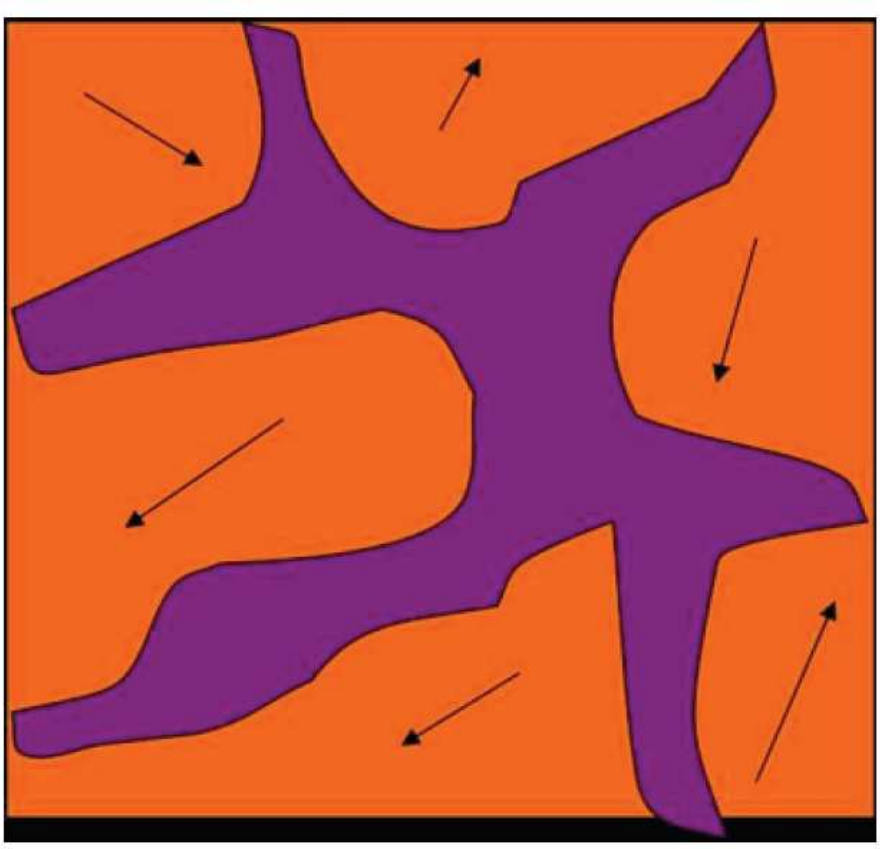

FIG. 31: FM islands(orange) with randomly oriented spins, separated by walls of competing insulating states(purple). Spins align themselves on application of magnetic field, walls melt and we get FM state

- Essential features of ferromagnetic metallic, FM, state are qualitatively understood using the DE ideas, though some work is required about the fine details of this state.

- The occurrence of charge/orbital ordered, CO, state has been predicted in Monte Carlo simulations and in the mean field studies of manganites. The model also shows the FM-CO competition which is essential for CMR.

- The existence of intrinsic inhomogeneties in single crystals have been established experimentally. Theoretical studies[67–71] including Monte Carlo simulations and mean field studies unveil phase separation both at mesoscopic as well as nanoscopic length scales.

- Theories based on states composed small FM islands with randomly oriented magnetizations appear to capture the essence of CMR physics([59, 72])(FIG. 31). The magnetizations in different FM domains align on application of magnetic field. The walls finally melt to give FM state with much lower resistivity and thus, CMR effect.

- Thoretical studies have predicted metallic and insulating phases separated by a first order transition[43].
- Both theoretical and experimental studies establishes a temperature, T^*, at which clusters start forming well above the Curie temperature.

B. Open Issues

- Why there is a paramagnetic insulator?
- Similar values for T_c and T_{CO}, temperature scales related to two totally different ground states.
- Microscopic bases for electronic inhomogeneties. Morover, why there are inhomogeneties at such wide length scales?
- Essence of phase separation for CMR effect. Careful experiments have to be performed to establish/destablish this idea.

V. OUTLOOK

Manganites are the fascinating class of materials which show phenonmenology as rich as any other field in condensed matter physics. The phases which they display are truly fascinating and existence of paramagnetic insulator, phase coexistence phenomenon etc. are phenomena almost exclusive to them. Almost all the degrees of freedom known in solid state physics are at play and fine interplay of interactions, close in energy, gives a complex phase diagram and extreme sensitivity to external stimulus. Electronic inhomogeneties in manganites seem unavoidable, showing probes in lot of experiments as reviewed in this article. But their theoretical understanding is far from complete.

Most of the thories on manganites integrate out all other DOFs (for example, oxygen ion, A-site cation) except those of Mn ions. Doped manganites have strain fields due to size mismatch of A-site cations. These long ranged strain fields included in any "reasonable" model for manganites should give mesoscopic phase separation. For example, $l-b$ model of Ramakrishnan et. al.[71] gives colossal response and $l-b$ model with long range coulomb interactions[73] give nanoscopic inhomogenities along with colossal response. Adding long ranged strain fields into $l-b$ model should give mesoscopic phase separation.

The important question is that whether electronic inhomogenities are necessary for CMR effect. There are theories which predicts CMR effect and produces the phase diagram essentially, without recourse to mesoscale inhomogeneties. There are references when CMR is displayed by manganites without showing any phase separation[74, 75], though in most other experiments known inhomogenities accompany the CMR effect. It seems that on the above grounds that electronic inhomogeneties are *not necessary* for CMR effect. Mesoscopic inhomogeneties might be because of effects like strain etc. More careful experiments are required to prove or disprove this.

---

[1] G. H. Jonker and J. H. Van Santen, Physica (Utrecht) **16**, 337 (1950).

[2] R. M. Kusters, J. Singleton, D. A. Keen, R. McGreevy, and W. Hayes, Physica B **155**, 362 (1989).

[3] R. von Helmolt, J. Wecker, B. Holzapfel, L. Schultz, and K. Samwer, Physical Review Letters **71**, 2331 (1993).

[4] S. Jin, T. H. Tiefel, M. McCormack, R. A. Fastnach, R. Ramesh, and L. H. Chen, Science **264**, 413 (1994).

[5] P. Schiffer, A. P. Ramirez, W. Bao, and S.-W. Cheong, Physical Review Letters **75**, 3336 (1995).

[6] J. C. Loudan, N. D. Mathur, and P. A. Midgley, Nature **420**, 797 (2002).

[7] C. N. R. Rao, A. K. Kundu, M. M. Seikh, and L. Sudheendra, Dalton Transactions pp. 3003–3011 (2004).

[8] N. Mathur and P. Littlewood, Physics Today **56**, 25 (2003).

[9] Y. Tokura and Y. Tomioka, Journal of Magnetism and Magnetic Materials **200**, 1 (1999).

[10] E. Dagotto, *Nanoscale Phase Separation and Colossal Magnetoresistance* (Springer-Verlag, Berlin, Germany, 2002).

[11] A. Moreo, S. Yunoki, and E. Dogotto, Science **283**, 2034 (1999).

[12] E. Dogotto, T. Hotta, and A. Moreo, Physics Reports **344**, 1 (2001).

[13] A. Ramirez, Journal of Physics : Condensed Matter **9**, 8171 (1997).

[14] J. Coey, M. Viret, and S. von Molnar, Advanced Physics **48**, 167 (1999).

[15] M. R. Ibarra and J. M. De Teresa, Materials Science Forum **302-303**, 125 (1999).

[16] C. N. R. Rao, A. Arulraj, A. K. Cheetham, and B. Raveau, Journal of Physics : Condensed Matter **12**, R83 (2000).

[17] A. Moreo, Journal of Electron Spectroscopy and Related Phenomena **117-118**, 251 (2001).

[18] M. B. Salamon and M. Jaime, Journal of Electron Spectroscopy and Related Phenomena **73**, 583 (2001).

[19] M. Imada, A. Fujimori, and Y. Tokura, Review of Modern Physics **70**, 1039 (1998).

[20] C. N. R. Rao and B. Raveau, eds., *Colossal Magnetoresistance, Charge Ordering, and Related Properties of Manganese Oxides* (World Scientific, Singapore, 1998).

[21] T. A. Kaplan and S. D. Mahanti, eds., *Physics of Manganites* (Kluwer/Plenum, NewYork, 1998).

[22] Y. Tokura, ed., *Colossal Magnetoresistive Oxides* (Gordon and Breach, London, 2000).

[23] A. Weisse and H. Fehske, New Journal of Physics **6**, 158 (2004).

[24] Y. Tokura, Reports on Progress in Physics **69**, 797 (2006).

[25] R. Hassan (2003), Dynamical Mean Field Theory of Falicov-Kimball and Related Models and their application to CMR Phenonmena in Manganites, Ph. D. Thesis, Indian Institute of Science.

[26] A. Urushibara, Y. Moritomo, T. Arima, A. Asamitsu, J. Kido, and Y. Tokura, Physical Review B **51**, 14103 (1995).

[27] H. Fujishiro, M. Ikebe, and Y. Konno, Journal of the Physical Society of Japan **67**, 1799 (1998).

[28] Y. Moritomo, T. Akimoto, A. Nakamura, K. Ohoyama, and M. Ohashi, Physical Review B **58**, 5544 (1998).

[29] Y. Yamada, O. Hino, S. Nohdo, R. Kanao, T. Inami, and S. Katano, Physical Review Letters **77**, 904 (1996).

[30] Y. Endoh, K. Hirota, S. Ishihara, S. Okamoto, Y. Murakami, A. Nishizawa, T. Fukuda, H. Kimura, H. Nojiri, K. Kaneko, et al., Physical Review Letters **82**, 4328 (1999).

[31] C. Zener, Physical Review **82**, 403 (1951).

[32] R. Kajimoto, H. Yoshizawa, H. Kawano, H. Kuwahara, Y. Tokura, K. Ohoyama, and M. Ohashi, Physical Review B **60**, 9506 (1999).

[33] Y. Tokura, Journal of the Physical Society of Japan **63**, 3931 (1994).

[34] A. Moreo, M. Mayr, A. Feiguin, S. Yunoki, and E. Dagotto, Physical Review Letters **84**, 5568 (2000).

[35] J. J. Neumeier, M. F. Hundley, J. D. Thompson, and R. H. Heffner, Physical Review B **52**, R7006 (1995).

[36] S.-W. Cheong and H. Hwang, *Contribution to Colossal Magnetoresistance Oxides, Monographs in Condensed Matter Science.* (Gordon and Breach, London, 1999).

[37] A. Ramirez, P. Schiffer, S.-W. Cheong, C. Chen, W. Bao, T. Palstra, P. Gammel, D. Bishop, and B. Zegarski, Physical Review Letters **76**, 3188 (1996).

[38] A. Millis, B. Shraiman, and P. Littlewood, Physical Review Letters **74**, 5144 (1995).

[39] G.-M. Zhao, K. Conder, H. Keller, and K. Muller, Nature **381**, 676 (1996).

[40] G.-M. Zhao, K. Conder, H. Keller, and K. Muller, Physical Review B **60**, 11914 (1999).

[41] T. Hotta and E. Dagotto, Physical Review B **61**, R11879 (2000).

[42] Z. Jirak, S. Krupicka, Z. Simsa, M. Dlouha, and Z. Vratislav, Journal of Magnetism and Magnetic Materials **53**, 153 (1985).

[43] Y. Tomioka and Y. Tokura, *Metal-insulator phenomena relevant to charge/orbital-ordering in perovskite-type manganese oxides.* (1999), prepint.

[44] Y. Tomioka, A. Asamitsu, H. Kuwahara, Y. Moritomo, and Y. Tokura, Physical Review B **53**, R1689 (1996).

[45] Y. Moritomo, H. Kuwahara, Y. Tomioka, and Y. Tokura, Physical Review B **55**, 7549 (1997).

[46] H. Kuwahara, Y. Tomioka, A. Asamitsu, Y. Moritomo, and Y. Tokura, Science **270**, 961 (1995).

[47] Y. Moritomo, Physical Review B **60**, 10374 (1999).

[48] T. Akimoto, Y. Maruyama, Y. Moritomo, A. Nakamura, K. Hirota, K. Ohoyama, and M. Ohashi, Physical Review B **57**, R5594 (1998).

[49] Y. Tomioka and Y. Tokura, Physical Review B **66**, 104416 (2002).

[50] H. Hwang, S.-W. Cheong, P. Radaelli, M. Marezio, and B. Batlogg, Physical Review Letters **75**, 914 (1995).

[51] E. a. Dagotto, Science **309**, 257 (2005).

[52] V. Shenoy, D. Sarma, and C. Rao, *Electronic phase separation in correlated oxides: The phenomenon, its present status and future prospects* (2006), preprint;to be published.

[53] P. Woodward, D. Cox, T. Vogt, and A. Cheetham, Chem. Mater. **11**, 3528 (1999).

[54] C. Ritter, R. Mahendiran, M. Ibarra, B. Morellon, A. ans Raveau, and C. Rao, Physical Review B **61**, R9229 (2000).

[55] L. Sudheendra and C. Rao, Journal of Physics: Condensed matter **18**, 3029 (2003).

[56] A. Kundu, M. Seikh, K. Ramesha, and C. Rao, Journal of Physics: Condensed matter **17**, 4171 (2005).

[57] S. Mori, C. Chen, and S.-W. Cheong, Nature **392**, 473 (1998).

[58] C. Renner, G. Aeppli, B. Kim, Y.-A. Soh, and S.-W. Cheong, Nature **416**, 518 (2002).

[59] M. Uehara, S. Mori, C. Chen, and S.-W. Cheong, Nature **399**, 560 (1999).

[60] M. Fath, S. Freisem, A. Menovsky, Y. Tomioka, J. Aarts, and J. Mydosh, Science **285**, 1540 (1999).

[61] L. Zhang, A. Israel, R. L. Greene, and A. de Lozanne, Science **298**, 805 (2002).

[62] P. Anderson and H. Hasegawa, Physical Review **100**, 675 (1955).

[63] P. Anderson, Physical Review **115**, 2 (1959).

[64] K. Kugel and D. Khomskii, Sov. Phys. JETP **37**, 725 (1974).

[65] E. Dagotto, New Journal of Physics **7**, 67 (2005).

[66] S. Yunoki, R. Hotta, and E. Dagotto, Physical Review Letters **84**, 3714 (2000).

[67] D. Arovas and F. Guinea, Physical Review B **58**, 9150 (1998).

[68] F. Guinea, G. GoH mez Santos, and D. Arovas, cond-mat **9907184** (1999).

[69] M. Kagan, D. Khomskii, and M. Mostovoy, The European Physical Journal B **12**, 217 (1999).

[70] D. Khomskii, cond-mat **0004034** (1999).

[71] T. V. Ramakrishnan, H. R. Krishnamurthy, S. Hassan, and G. V. Pai, cond-mat **0308396** (2003).

[72] J. Burgy, M. Mayr, V. Martin-Mayor, A. Moreo, and E. Dagotto, Physical Review Letters **87**, 277202 (2001).

[73] V. Shenoy, T. Gupta, H. R. Krishnamurthy, and T. Ramakrishnan, *Coulomb interactions and nanoscale electronic inhomogeneities* (2006), prepint; to be published.

[74] R. Mathieu, D. Akahoshi, A. Asamitsu, Y. Tomioka, and Y. Tokura, Physical Review Letters **93**, 227202 (2004).

[75] V. Moshnyaga, L. Sudheendra, O. I. Lebedev, K. Gehrke, O. Shapova, A. Belenchuk, S. Koster, B. Dam-

aschke, G. van Tendeloo, and K. Samwer, cond-mat **0512350** (2005).